PCT WORLD INTELLECTUAL PROPERTY ORGANIZATION
International Bureau

INTERNATIONAL APPLICATION PUBLISHED UNDER THE PATENT COOPERATION TREATY (PCT)

(51) International Patent Classification 7 : H04B

A2

(11) International Publication Number: **WO 00/49720**

(43) International Publication Date: 24 August 2000 (24.08.00)

(21) International Application Number: PCT/FI00/00119

(22) International Filing Date: 16 February 2000 (16.02.00)

(30) Priority Data:
990316 16 February 1999 (16.02.99) FI

(71) Applicant *(for all designated States except US)*: JYVÄSKYLÄN TEKNOLOGIAKESKUS OY [FI/FI]; P.O. Box 27, FIN–40101 Jyväskylä (FI).

(72) Inventors; and
(75) Inventors/Applicants *(for US only)*: RISTANIEMI, Tapani [FI/FI]; Keljonkankaantie 52 A 2, FIN–40530 Jyväskylä (FI). JOUTSENSALO, Jyrki [FI/FI]; Keskustie 22 A 4, FIN–40100 Jyväskylä (FI).

(74) Agent: BERGGREN OY AB; P.O. Box 16, FIN–00101 Helsinki (FI).

(81) Designated States: AE, AL, AM, AT, AU, AZ, BA, BB, BG, BR, BY, CA, CH, CN, CR, CU, CZ, DE, DK, DM, EE, ES, FI, GB, GD, GE, GH, GM, HR, HU, ID, IL, IN, IS, JP, KE, KG, KP, KR, KZ, LC, LK, LR, LS, LT, LU, LV, MA, MD, MG, MK, MN, MW, MX, NO, NZ, PL, PT, RO, RU, SD, SE, SG, SI, SK, SL, TJ, TM, TR, TT, TZ, UA, UG, US, UZ, VN, YU, ZA, ZW, ARIPO patent (GH, GM, KE, LS, MW, SD, SL, SZ, TZ, UG, ZW), Eurasian patent (AM, AZ, BY, KG, KZ, MD, RU, TJ, TM), European patent (AT, BE, CH, CY, DE, DK, ES, FI, FR, GB, GR, IE, IT, LU, MC, NL, PT, SE), OAPI patent (BF, BJ, CF, CG, CI, CM, GA, GN, GW, ML, MR, NE, SN, TD, TG).

Published
Without international search report and to be republished upon receipt of that report.

(54) Title: METHOD FOR SYNCHRONIZATION IN A SPREAD SPECTRUM RECEIVER

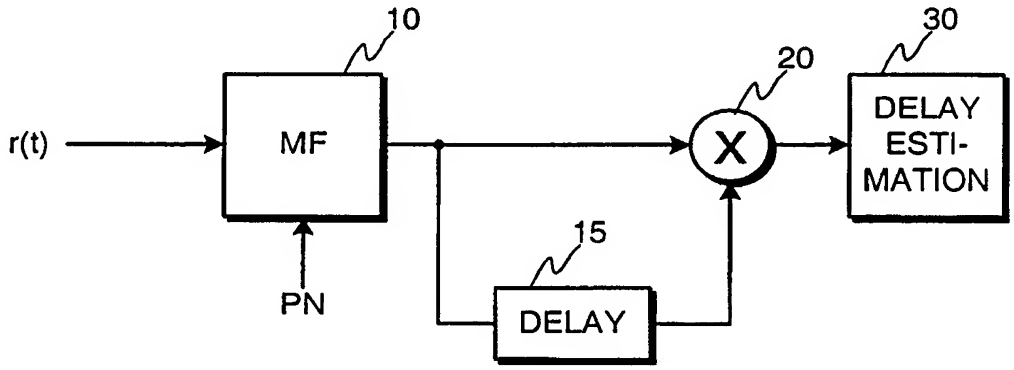

(57) Abstract

The invention relates to synchronization methods for spread spectrum receivers. The invention provides improved synchronization methods based on the use of differential correlation.

FOR THE PURPOSES OF INFORMATION ONLY

Codes used to identify States party to the PCT on the front pages of pamphlets publishing international applications under the PCT.

AL	Albania	**ES**	Spain	**LS**	Lesotho	**SI**	Slovenia
AM	Armenia	**FI**	Finland	**LT**	Lithuania	**SK**	Slovakia
AT	Austria	**FR**	France	**LU**	Luxembourg	**SN**	Senegal
AU	Australia	**GA**	Gabon	**LV**	Latvia	**SZ**	Swaziland
AZ	Azerbaijan	**GB**	United Kingdom	**MC**	Monaco	**TD**	Chad
BA	Bosnia and Herzegovina	**GE**	Georgia	**MD**	Republic of Moldova	**TG**	Togo
BB	Barbados	**GH**	Ghana	**MG**	Madagascar	**TJ**	Tajikistan
BE	Belgium	**GN**	Guinea	**MK**	The former Yugoslav Republic of Macedonia	**TM**	Turkmenistan
BF	Burkina Faso	**GR**	Greece			**TR**	Turkey
BG	Bulgaria	**HU**	Hungary	**ML**	Mali	**TT**	Trinidad and Tobago
BJ	Benin	**IE**	Ireland	**MN**	Mongolia	**UA**	Ukraine
BR	Brazil	**IL**	Israel	**MR**	Mauritania	**UG**	Uganda
BY	Belarus	**IS**	Iceland	**MW**	Malawi	**US**	United States of America
CA	Canada	**IT**	Italy	**MX**	Mexico	**UZ**	Uzbekistan
CF	Central African Republic	**JP**	Japan	**NE**	Niger	**VN**	Viet Nam
CG	Congo	**KE**	Kenya	**NL**	Netherlands	**YU**	Yugoslavia
CH	Switzerland	**KG**	Kyrgyzstan	**NO**	Norway	**ZW**	Zimbabwe
CI	Côte d'Ivoire	**KP**	Democratic People's Republic of Korea	**NZ**	New Zealand		
CM	Cameroon			**PL**	Poland		
CN	China	**KR**	Republic of Korea	**PT**	Portugal		
CU	Cuba	**KZ**	Kazakstan	**RO**	Romania		
CZ	Czech Republic	**LC**	Saint Lucia	**RU**	Russian Federation		
DE	Germany	**LI**	Liechtenstein	**SD**	Sudan		
DK	Denmark	**LK**	Sri Lanka	**SE**	Sweden		
EE	Estonia	**LR**	Liberia	**SG**	Singapore		

Method for synchronization in a spread spectrum receiver

BACKGROUND OF THE INVENTION

1. Field of the Invention

The invention relates to synchronization methods for spread spectrum receivers. Especially, the invention is related to such a method as specified in the preamble of claim 1.

2. Description of Related Art

Wideband Code Division Multiple Access (WCDMA or CDMA) technology is a strong candidate for future global wireless mobile communications. WCDMA [1] has been selected as an air interface solution e.g. in UMTS (Universal Mobile Telecommunication System) standard, which will provide a multitude of services, especially multimedia and high bit rate packet data.

CDMA is based on spread sprectum technique, where the idea is to spread the narrowband information signal into a common wide frequency band before transmission. In Direct Sequence (DS) CDMA, the spreading is performed by wideband noise-like signal, which simultaneously identifies each user in the system. This pseudo-noise is also called the code or the chip sequence of a particular user.

The final objective in the reception of a DS-CDMA system is to estimate the symbols which carry the data, but a prerequisite task is to get the local code generator synchronized to that of received signal. This means estimation of the propagation delay, which gives the required knowledge to the receiver about the phase of the spreading code. In addition, the strengths of possible multipaths, and carrier phase must be estimated. Code timing estimation tends to be the most challenging task, and the other parameters can be estimated given a reliable delay estimate [2,3].

Conventional CDMA systems rely on single-user techniques, such as matched filter [4], in both delay estimation and detection. Although simple, they are inadequate if the code orthogonality conditions are perturbed. This happens even in synchronous system with orthogonal codes due to the existence of multipaths with different

delays. Moreover, if the desired signal is much weaker than the interfering signals, which is commonly known as a near-far problem, single-user techniques can totally collapse. In the uplink (e.g. mobile to base) communication, near-far problem can be mitigated by power control, but if used in downlink (e.g. base to mobile) communications, it actually causes near-far effect for the downlink receiver. This is the case e.g. in the WCDMA concept, where equal performance is offered to each mobile user, regardless of their locations. The work of Verdú [5] meant, however, that it is possible to eliminate the effects of multiple access interference and near-far problem. This optimum multiuser detector, although computationally demanding and requires all the system parameters to be known, initiated the development of lower complexity near-far resistant techniques for both detection [6,7] and delay/channel estimation [8,9].

Code timing acquisition refers to coarse delay estimation, where the maximal acceptable error is half a chip duration. In [8,9] a subspace approach was considered, which was based on multiple signal classification (MUSIC) [12]. However, their performance is found to be inadequate in highly loaded systems [10], when the signal might not have subspace structure anymore. Since acquisition takes place before actual data transmission, training symbols or preamble can be used. This was utilized in [10] and [11]. Both maximum likelihood -based algorithms modeled the training symbols as desired signal and all the interference as colored non-Gaussian noise that is uncorrelated with the desired signal. The algorithm in [10] was found to be near-far resistant and tolerate high system loading. In addition, the accuracy of the delay estimate was achieved by solving a second-order polynomial for each chip interval. A major limitation, however, is that the method can not be extended to fading channels. This is mainly because of the need of long training period, during which the channel may have a (sample) mean too close to zero. This disadvantage was removed by receiver diversity in [13], which allowed shorter training. The algorithm in [11] also has limitations in extension to the fading channels, and moreover looses its near-far resistance in highly loaded systems. The computational complexity of all those algorithms is also still quite high from the downlink signal processing point of view. Most promising performance with low computation was found in [14], where the effects of interference were suppressed by correlating the matched filter output with a delayed version of it. The motivation for this differential correlation is roughly speaking as follows: when only +1's are sent to desired user, its contribution in the received signal at the symbol level is only the fading process, whose time-correlatedness can be exploited. Basically the same idea was exploited also in [15], with the exception that the differential correlation was

performed prior to matched filtering. This was due to the special shift-and-add -property of *m*-sequences, which makes the proposed algorithm sensitive to the choice of spreading code.

SUMMARY OF THE INVENTION

An object of the invention is to realize a synchronization method, which alleviates the problems associated with the prior art. A further object of the invention is to realize a synchronization method, which is more interference tolerant than the prior art methods.

The objects are reached by exploiting differential correlation.

The method according to the invention is characterized by that, which is specified in the characterizing part of the independent method claim. The dependent claims describe further advantageous embodiments of the invention.

BRIEF DESCRIPTION OF THE DRAWINGS

Various embodiments of the invention will be described in detail below, by way of example only, with reference to the accompanying drawings, of which

Figure 1 illustrates a channel model used in the description of an advantageous embodiment of the invention,

Figure 2 illustrates a part of a block diagram of a spread spectrum receiver based on non-coherent matched filtering according to prior art and a part of a block diagram of a spread spectrum receiver based on non-coherent differentially correlated matched filtering according to the invention,

Figure 3 illustrates an example of a typical fading process,

Figure 4 illustrates the results of a comparison simulation of probability of acquisition with inventive and prior art synchronization methods,

Figure 5 illustrates the results of a further comparison simulation of probability of acquisition with inventive and prior art synchronization methods,

Figure 6 illustrates the results of a comparison simulation of mean acquisition times with inventive and prior art synchronization methods,

Figure 7 illustrates the results of a further comparison simulation of mean acquisition times with inventive and prior art synchronization methods,

Figure 8 illustrates the results of a comparison simulation of number of acquired paths with inventive and prior art synchronization methods,

Figure 9 illustrates the results of a comparison simulation of probability of acquisition as a function of number of users with inventive and prior art synchronization methods,

Figure 10 illustrates the results of a comparison simulation of mean acquisition time as a function of number of users with inventive and prior art synchronization methods,

Figure 11 illustrates the results of a comparison simulation of probability of acquisition as a function of number of paths with inventive and prior art synchronization methods,

Figure 12 illustrates the results of a comparison simulation of RMSE as a function of number of users with inventive and prior art synchronization methods,

Figure 13 illustrates the results of a comparison simulation of RMSE as a function of preamble length with inventive and prior art synchronization methods,

Figure 14 illustrates a block diagram of a part of a receiver according to an advantageous embodiment of the invention, and

Figure 15 illustrates a block diagram of a part of a receiver according to a further advantageous embodiment of the invention.

DETAILED DESCRIPTION OF THE PREFERRED EMBODIMENTS

According to a further aspect of the invention, simple and efficient algorithms for the code timing acquisition in the Direct-Sequence Code-Division Multiple Access (DS-CDMA) communication system. The essential assumption is that a preamble is available for the desired user. Then the correlation matrix $\mathbf{R}(\tau)$ of the sampled data, where τ is suitably chosen time lag, contains the timing information only of desired user, while the contributions of uncorrelated interferers and noise are suppressed out. Coarse delay estimates are then obtained by matched filter (MF) or multiple signal classification (MUSIC)-type approaches. In the latter case only L eigenvectors are computed, where L is the number of resolvable paths. For cases in which only one path exists, an additional procedure is proposed to both approaches, by which the estimation accuracy is greatly improved with neglible increase in computation. More precisely, the chip timing offset due to chip-asyncronous sampling can be determined by solving a system of two second-order polynomials for each chip interval. Therefore, only at most $2C$ hypotheses are needed, where C is the processing gain. All the proposed methods are computationally quite simple, containing mainly MF-operations, or at most computation of only few eigenvectors. Numerical experiments speaks for the possibility of achieving significant performance gains compared to conventional acquisition, making them attractive options to be attached for the next generation mobile receivers.

The present aspect of the invention brings several improvements over [14]. According to the present aspect of the invention, we assume periodic (or "short") spreading codes, and analyze the properties of the correlation matrix of the received and sampled data with non-zero time lags. In short, we call it a differential correlation matrix. In addition, two extentions are made. First, the assumption of periodic codes makes it possible to consider also eigenvalue-based approaches. We do this by applying MUSIC [12], which has also earlier been applied to CDMA synchronization in [8, 9]. In those papers, however, MUSIC was applied to the data correlation

matrix with *zero* time lag, and problems arose in high system loads due to the disappearance of signal subspace structure. According to the present aspect of the invention, it is reasonable to apply MUSIC even in highly loaded systems, because differential correlations effectively filters interference prior to actual delay estimation. Therefore, the signal subspace dimension is significantly reduced while still preserving the desired information, making the circumstances favorable for MUSIC. Second, we assume arbitrary delays, and propose a simple way to accurately estimate the chip timing offset in single-path case. This is an important task since the estimation errors in chip timings may cause serious performance losses in symbol estimation [16]. The invention enables determining the fractional part of the delay by solving a system of two second-order polynomials for each chip interval.

1. PROBLEM FORMULATION

1.1 NOTATIONS

Throughout the paper, lower and upper case boldface letters denote vectors and matrices, respectively. In addition, we denote

$(\cdot)^*$	complex conjugate
$(\cdot)^T$,$(\cdot)^H$	transpose, and Hermitian transpose
$E\{\cdot\}$	expected value
sign$\{\cdot\}$	sign-function
$\mathbf{x}_n$	nth vector
$\|\|\cdot\|\|$	Frobenius norm
$\mathbf{0}, \mathbf{1}$	matrices with all entries 0 and 1, respectively

1.2 SIGNAL MODEL

The signal model studied in this paper is a baseband downlink model with fading multipath channel, and additive white gaussian noise. The channel model is depicted

in Figure 1, where the signal sent by the base station is $x(t) = \sum_{m=1}^{M} \sum_{k=1}^{K} b_{km} s_k(t - mT)$, containing the information of M symbols of K users. Here b_{km} is kth user's mth symbol, $s_k(\cdot)$ is kth user's chip sequence. $s_k(t) \in \{-1, +1\}$, $t \in [0, T)$, $s_k(t) = 0$, $t \notin [0, T)$, where T is the symbol duration. We assume that the channel is fixed during one symbol, i.e. $a_l(t) = a_{lm}, t \in [mT, (m+1)T)$ in the Figure 1. a_{lm} is called an attenuation factor of the lth path, which a complex number and may vary symbol by symbol. The received signal hence have the form

$$r(t) = \sum_{m=1}^{M} \sum_{k=1}^{K} b_{km} \sum_{l=1}^{L} a_{lm} s_k(t - mT - \chi_l T_c) + n(t), \tag{1}$$

where L is the number of resolvable paths, T_c is the chip duration, and $\chi_l T_c$ is the delay of the lth path, where $\chi_l = d_l + \delta_l$ with d_l integer and $\delta_l \in [0, 1)$. The delay of each path is assumed to remain roughly constant in the observation interval. $n(t)$ denotes noise, and the chip sequence length (i.e. processing gain) is $C = \frac{T}{T_c}$. From now on, we assume $T_c = 1$ for simplicity.

First, the received data is sampled by chip-matched filtering, and the equispaced samples are collected into C-vectors $\mathbf{r}_m$,

$$\mathbf{r}_m = [r[mC], r[mC+1], \cdots, r[mC+C-1]]^T. \tag{2}$$

They have the well known form (e.g. [8])

$$\mathbf{r}_m = \sum_{k=1}^{K} \sum_{l=1}^{L} [a_{l,m-1} b_{k,m-1} \underline{\mathbf{c}}_{kl} + a_{lm} b_{km} \overline{\mathbf{c}}_{kl}] + \mathbf{n}_m, \tag{3}$$

where $\mathbf{n}_m$ denotes noise vector, and

$$\underline{\mathbf{c}}_{kl} = \underline{\mathbf{c}}_{kl}(\chi_l) = (1 - \delta_l) \underline{\mathbf{g}}_{kl}(d_l) + \delta_l \underline{\mathbf{g}}_{kl}(d_l + 1) \tag{4}$$

$$\overline{\mathbf{c}}_{kl} = \overline{\mathbf{c}}_{kl}(\chi_l) = (1 - \delta_l) \overline{\mathbf{g}}_{kl}(d_l) + \delta_l \overline{\mathbf{g}}_{kl}(d_l + 1). \tag{5}$$

Here the "early" and "late" parts of the code vectors are

$$\underline{\mathbf{g}}_{kl}(d_l) = \begin{bmatrix} s_k[C - d_l + 1] & \cdots & s_k[C] & 0 & \cdots & 0 \end{bmatrix}^T \tag{6}$$

$$\overline{\mathbf{g}}_{kl}(d_l) = \left[\begin{array}{cccccc} 0 & \cdots & 0 & s_k[1] & \cdots & s_k[C-d_l] \end{array} \right]^T. \quad (7)$$

Notice that Eqs. (4)-(5) and (6)-(7) are due to chip and symbol asyncronous sampling, respectively. To get more compact representation of the data, define a $C \times 2KL$ dimensional code matrix $\mathbf{G}$,

$$\mathbf{G} \stackrel{\text{def}}{=} [\underline{\mathbf{c}}_{11}, \overline{\mathbf{c}}_{11}, \ldots, \underline{\mathbf{c}}_{1L}, \overline{\mathbf{c}}_{1L}, \ldots, \underline{\mathbf{c}}_{KL}, \overline{\mathbf{c}}_{KL}], \quad (8)$$

and a 2-vector

$$\mathbf{z}_{klm} = [a_{l,m-1}b_{k,m-1}, a_{lm}b_{km}]^T. \quad (9)$$

Stacking all vectors $\mathbf{z}_{klm}$ into a $2KL$-vector $\mathbf{a}_m$,

$$\mathbf{a}_m = [\mathbf{z}_{11m}^T, \ldots, \mathbf{z}_{1Lm}^T, \ldots, \mathbf{z}_{KLm}^T]^T, \quad (10)$$

the sample vector (3) can be rewritten as

$$\mathbf{r}_m = \mathbf{G}\mathbf{a}_m + \mathbf{n}_m. \quad (11)$$

Here $\mathbf{G}$ depends on the codes and the delays, and $\mathbf{a}_m$ depends on the channel coefficients and the symbols.

2. SYNCHRONIZATION ALGORITHMS

Our goal is to compute the correlation matrix $\mathbf{R}(\tau)$ of the sampled data (11), where the time lag equals $\tau \neq 0$ symbols. In short, we call $\mathbf{R}(\tau)$ a differential- instead of autocorrelation matrix to stress the nonzero time lag. The proposed methods are based on the observation that $\mathbf{R}(\tau)$ contains timing information only of the desired user, which is first shown. The following realistic assumptions are made:

#1. A constant preamble $b_{1m} = 1, m = 1, \ldots, M$ ("all ones") is available for the desired user, which is the user $k = 1$ from now on.

#2. Symbols of interfering users are uncorrelated random binary variables of zero mean. Then $E\{b_{km}b_{k',m+\tau}\} = 0$, and $E\{b_{km}\} = 0$ for $k \neq 1$.

#3. Fading processes of each path are uncorrelated and zero mean. Then $E\{a_{lm}a^*_{l'n}\} = 0$ for $l \neq l'$, and $E\{a_{lm}\} = 0$.

#4. Fading process of each path is stationary. Therefore, the correlation coefficient equals
$\alpha_l(\tau) \stackrel{\text{def}}{=} \frac{E\{a_{lm}a^*_{ln}\}}{E\{|a_{lm}|\}E\{|a^*_{ln}|\}} = \frac{E\{a_{lm}a^*_{ln}\}}{\mu_l^2}$, where $\tau = m - n$, and $\mu_l = E\{|a_{lm}|\}$.

#5. Noise is a random zero mean variable, and independent with the data and fading. Then $E\{\mathbf{n}_m\mathbf{n}^H_{m+\tau}\} = \mathbf{0} = E\{\mathbf{n}_m\mathbf{a}^H_{m+\tau}\}$, where $\mathbf{n}_m$ and $\mathbf{a}_m$ are those of Eq. (11).

Notice that assumptions (#3) and (#4), without zero-mean assumption, are equivalent to the common uncorrelated scatterer (US) model [4], and wide-sense stationary (WSS) model [18], respectively. It should be noted, however, that assumption (#3) is not necessary for the purposes of the paper, but it is made to achieve a simple and elegant representation of $\mathbf{R}(\tau)$. The case where (#3) do not apply is discussed in **Remark 1.**

According to Eq. (11), and assumption (#5), the differential correlation matrix now is

$$\begin{aligned}\mathbf{R}(\tau) \stackrel{\text{def}}{=} E\{\mathbf{r}_m\mathbf{r}^H_{m+\tau}\} &= E\{(\mathbf{G}\mathbf{a}_m + \mathbf{n}_m)(\mathbf{G}\mathbf{a}_{m+\tau} + \mathbf{n}_{m+\tau})^H\} \\ &= \mathbf{G}\mathbf{A}(\tau)\mathbf{G}^T, \end{aligned} \tag{12}$$

where the $2KL \times 2KL$ dimensional matrix $\mathbf{A}(\tau)$ is defined as

$$\mathbf{A}(\tau) \stackrel{\text{def}}{=} E\{\mathbf{a}_m\mathbf{a}^H_{m+\tau}\}. \tag{13}$$

According to Eq. (10), the matrix $\mathbf{A}(\tau)$ contains $(KL)^2$ submatrices of dimension 2×2. Denote these by $\mathbf{A}_{(kl),(k'l')}(\tau)$, i.e.

$$\mathbf{A}_{(kl),(k'l')}(\tau) \stackrel{\text{def}}{=} E\{\mathbf{z}_{klm}\mathbf{z}^H_{k'l',m+\tau}\}. \tag{14}$$

From Eq. (9) we directly have

$$\mathbf{A}_{(kl),(k'l')}(\tau) = E\{\left[\begin{array}{c|c} a_{l,m-1}a^*_{l',m+\tau-1}b_{k,m-1}b_{k',m+\tau-1} & a_{l,m-1}a^*_{l',m+\tau}b_{k,m-1}b_{k',m+\tau} \\ a_{lm}a^*_{l',m+\tau-1}b_{km}b_{k',m+\tau-1} & a_{lm}a^*_{l',m+\tau}b_{km}b_{k',m+\tau} \end{array}\right]\}. \tag{15}$$

Since fading and symbol processes are independent, we have moreover

$$\mathbf{A}_{(kl),(k'l')}(\tau) = \left[\begin{array}{c|c} E\{a_{l,m-1}a^*_{l',m+\tau-1}\}E\{b_{k,m-1}b_{k',m+\tau-1}\} & E\{a_{l,m-1}a^*_{l',m+\tau}\}E\{b_{k,m-1}b_{k',m+\tau}\} \\ E\{a_{lm}a^*_{l',m+\tau-1}\}E\{b_{km}b_{k',m+\tau-1}\} & E\{a_{lm}a^*_{l',m+\tau}\}E\{b_{km}b_{k',m+\tau}\} \end{array}\right]. \tag{16}$$

We next show that almost all matrices $\mathbf{A}_{(kl),(k'l')}(\tau)$ are equal to $\mathbf{0}$, provided the time difference is equal to $\tau = 2$ symbols or more. The reason why $\tau = 1$ is not a good choice for the time lag is discussed in **Remark 2**.

Case 1: $1 = k = k'$. Now all the symbols are equal to 1, and $\mathbf{A}_{(1l),(1l')}(\tau)$ depends only on the channel coefficients. With $l \neq l'$ we have $\mathbf{A}_{(1l),(1l')}(\tau) = \mathbf{0}$ due to assumption (#3). On the other hand, with $l = l'$, we have due to assumption (#4)

$$\mathbf{A}_{(1l),(1l)}(\tau) = \mu_l^2 \left[\begin{array}{cc} \alpha_l(\tau) & \alpha_l(\tau+1) \\ \alpha_l(\tau-1) & \alpha_l(\tau) \end{array}\right]. \tag{17}$$

Case 2: $1 = k \neq k'$. Now $\mathbf{A}_{(1l),(k'l')}(\tau)$ depends on the channel coefficients and the symbols of user k'. Since these symbols are zero mean, $\mathbf{A}_{(1l),(k'l')}(\tau) = \mathbf{0}$ for all l, l'.

Case 3: $1 \neq k, k'$. In this case, we always have $\mathbf{A}_{(kl),(k'l')}(\tau) = \mathbf{0}$ due to assumption (#2).

Hence, the matrix $\mathbf{A}(\tau)$ contains only L non-zero submatrices of 2×2, and they correspond to situations where $k = k' = 1$ and $l = l'$. Due to the definition of

Eq. (10), these submatrices are situated in the main diagonal of $\mathbf{A}(\tau)$. Eq. (12) therefore reduces to

$$\mathbf{R}(\tau) = \mathbf{G} \left[\begin{array}{ccc|c} \mathbf{A}_{(11),(11)}(\tau) & & \mathbf{0} & \\ & \ddots & & \mathbf{0} \\ \mathbf{0} & & \mathbf{A}_{(1L),(1L)}(\tau) & \\ \hline & \mathbf{0} & & \mathbf{0} \end{array}\right] \mathbf{G}^T, \tag{18}$$

from which we see that $\mathbf{R}(\tau)$ depends only on $2L$ first rows of the codematrix $\mathbf{G}$. Since these rows correspond to the desired user $k = 1$ only, see Eq. (8), the contribution of interference is suppressed from $\mathbf{R}(\tau)$. To express in detail the form of $\mathbf{R}(\tau)$, we make a mild assumption that $\alpha_l(\tau - 1) \approx \alpha_l(\tau) \approx \alpha_l(\tau + 1)$, and denote it $\bar{\alpha}_l(\tau)$. This means that the fading process has almost the same degree of correlation whether the time difference is $\tau - 1, \tau$ or $\tau + 1$ symbols. Then, Eq.(17) reduces to $\mathbf{A}_{(1l),(1l)}(\tau) = \mu_l^2 \bar{\alpha}_l(\tau)\mathbf{1}$, and consequently (see details in the Appendix A)

$$\mathbf{R}(\tau) = \mathbf{G} \left[\begin{array}{ccc|c} \mu_1^2\bar{\alpha}_1(\tau)\mathbf{1} & & \mathbf{0} & \\ & \ddots & & \mathbf{0} \\ \mathbf{0} & & \mu_L^2\bar{\alpha}_L(\tau)\mathbf{1} & \\ \hline & \mathbf{0} & & \mathbf{0} \end{array}\right] \mathbf{G}^T = \sum_{l=1}^{L} \mu_l^2 \bar{\alpha}_l(\tau)\mathbf{c}_{1l}\mathbf{c}_{1l}^T, \tag{19}$$

where

$$\mathbf{c}_{1l} \stackrel{\text{def}}{=} \underline{\mathbf{c}}_{1l} + \overline{\mathbf{c}}_{1l}. \tag{20}$$

From the structure of $\mathbf{R}(\tau)$ we see explicitly that it contains the code and delay information of the desired user $k = 1$ only.

Remark 1. The reason for assumption (#3) was to achieve a compact representation Eq. (19). However, to ensure that the differential correlation matrix $\mathbf{R}(\tau)$, with $\tau \geq 2$ symbols, contains *only* the desired user's information, assumption (#3) is not necessary. This is because the contribution of interfering users are got only via "Case 2" and "Case 3" above. However, in those cases the zero submatrices were

always due to the uncorrelatedness and zero-mean properties of the interfering user's symbols. Therefore, $\mathbf{R}(\tau)$ is free of contributions of interfering users even without assumption (#3), although the form of $\mathbf{R}(\tau)$ is little bit different. This is because now in "Case 1", both subcases "$l = l'$", and "$l \neq l'$" cause non-zero submatrices. Assumption (#3) is valid e.g. for Rayleigh-fading channels [4], but do not apply e.g. for Rician fading [4] and fixed multipath channels. In the former case, the paths are uncorrelated but non-zero mean, whereas in the latter case, the paths are both correlated and non-zero mean.

Remark 2. It is important to notice, that the situation $\tau = 1$ is not as desired as the case $\tau \geq 2$ symbols. The reason is as follows: due to symbol asyncronous sampling, the sample vectors $\mathbf{r}_m$ usually contain information about two successive symbols, see Eq. (3). Therefore, with the time lag $\tau = 1$ symbol, two successive sample vector have some degree of correlation also with respect to the interfering users. To see this in detai, let $\tau = 1$, and consider

$$\mathbf{A}_{(kl),(k'l')}(1) = \left[\begin{array}{c|c} E\{a_{l,m-1}a^*_{l'm}\}E\{b_{k,m-1}b_{k'm}\} & E\{a_{l,m-1}a^*_{l',m+1}\}E\{b_{k,m-1}b_{k',m+1}\} \\ E\{a_{lm}a^*_{l'm}\}E\{b_{km}b_{k'm}\} & E\{a_{lm}a^*_{l',m+1}\}E\{b_{km}b_{k',m+1}\} \end{array}\right]. \tag{21}$$

If now $1 \neq k = k'$ with $l = l'$, which belongs to the "Case 3" above, we would have a non-zero submatrix equal to

$$\mathbf{A}_{(kl),(kl)}(1) = \left[\begin{array}{cc} 0 & 0 \\ E\{|a_{lm}|^2\} & 0 \end{array}\right]. \tag{22}$$

If $\mathbf{R}(1)$ is now rewritten in the form of Eq. (19), $\mathbf{R}(1)$ would clearly have a contribution which corresponds to the interfering user $k \neq 1$. For this reason, we consider only cases where $\tau \geq 2$ symbols.

Remark 3. It is worth mentioning that the differential correlation matrix $\mathbf{R}(\tau)$ with $\tau \geq 2$ contains two kinds of information about the channel: the average powers

of the paths, and the rapidity of their fading processes. The latter is related to the correlation coefficient $\bar{\alpha}_l(\tau)$, which is the closer to 0 (resp. 1) the faster (resp. slower) is the fading process. Therefore, provided equienergy paths, the slowly varying paths are the best represented in $\mathbf{R}(\tau)$. This is a nice property, because such paths are more valuable to be acquired due to their easier tracking.

2.1 MF-TYPE APPROACH

In practice $\mathbf{R}(\tau)$ is estimated by $\hat{\mathbf{R}}(\tau) = \frac{1}{M}\sum_{m=1}^{M} \mathbf{r}_m \mathbf{r}_{m+\tau}^H$. The simplest way to estimate the delay is try to match the known code to the data as well as possible, i.e. to find the solution for

$$\hat{\chi} = \arg\max_{\chi} \frac{|\mathbf{c}_1(\chi)^T \hat{\mathbf{R}}(\tau)\mathbf{c}_1(\chi)|}{\|\mathbf{c}_1(\chi)\|^2}. \tag{23}$$

Here $\mathbf{c}_1(\chi)$ is a replica of the user's $k = 1$ code, corresponding to the fractional testdelay $\chi = d + \delta$. Formally,

$$\mathbf{c}_1(\chi) \stackrel{\text{def}}{=} (1-\delta)\mathbf{g}_1(d) + \delta\mathbf{g}_1(d+1) \tag{24}$$

$$\stackrel{\text{def}}{=} (1-\delta)\begin{bmatrix} s_1[C-d+1] & \cdots & s_1[C] & s_1[1] & \cdots & s_1[C-d] \end{bmatrix}^T + \delta\begin{bmatrix} s_1[C-d] & \cdots & s_1[C] & s_1[1] & \cdots & s_1[C-d-1] \end{bmatrix}^T \tag{25}$$

The delay estimator Eq. (23), which we label DC-MF (Differential Correlations based MF), was the main contribution of our earlier work [19]. Notice that as "all ones" preamble is used, the conventional non-coherent MF is exactly DC-MF with $\tau = 0$. It is also worth to notice that, since Eq. (23) equals

$$\hat{\chi} = \arg\max_{\chi} \left|\frac{1}{M}\sum_{m=1}^{M} \frac{\mathbf{c}_1(\chi)^T \mathbf{r}_m}{\|\mathbf{c}_1(\chi)\|} \frac{\mathbf{r}_{m+\tau}^H \mathbf{c}_1(\chi)}{\|\mathbf{c}_1(\chi)\|}\right|, \tag{26}$$

DC-MF includes, indeed, only MF and delay operations. Estimator of form Eq. (26) would be the practical implementation of DC-MF, and is depicted in Figure 2.

2.2 MUSIC-TYPE APPROACH

In practice, the estimate $\hat{\mathbf{R}}(\tau)$ will always contain some contributions of interfering users and noise due to the finite length of the preamble. But if $\hat{\mathbf{R}}(\tau)$ would have exactly the form of Eq. (12), or equally Eq. (19), it could be rewritten by eigenvalue decomposition as

$$\mathbf{R}(\tau) = \mathbf{U}(\tau)\mathbf{\Lambda}\mathbf{U}(\tau)^T. \tag{27}$$

Here $\mathbf{\Lambda}$ is a diagonal matrix, whose diagonal elements are L non-zero eigenvalues of $\mathbf{R}(\tau)$, and $\mathbf{U}(\tau)$ is a $C \times L$ dimensional matrix, containing the related eigenvectors on its columns. But then MUSIC (MUltiple SIgnal Classification) [12] could be used to estimate the delays. Due to finite number of samples, $\hat{\mathbf{R}}(\tau)$ will be in practice asymmetric, and it must be first symmetrized to achieve real eigenvalues and orthonormal eigenvectors. Therefore, we define symmetric $\hat{\mathbf{R}}_{\text{sym}}(\tau) = \hat{\mathbf{R}}(\tau) + \hat{\mathbf{R}}(\tau)^H$, for which MUSIC is applied. More precisely, the delay estimation is performed as

$$\hat{\chi} = \arg\max_{\chi} \frac{\|\hat{\mathbf{U}}^T(\tau)\mathbf{c}_1(\chi)\|^2}{\|\mathbf{c}_1(\chi)\|^2}, \tag{28}$$

where $\hat{\mathbf{U}}(\tau)$ consists of L principal eigenvectors of $\hat{\mathbf{R}}_{\text{sym}}(\tau)$. We label this estimator as DC-MUSIC (Differential Correlations based MUSIC).

MUSIC has been applied to CDMA chip timing acquisition also earlier in [8, 9], but it should be stressed that DC-MUSIC is totally different from those. This is because in those papers MUSIC was applied to the data correlation matrix $\hat{\mathbf{R}}(0)$. Formally, as the preamble is "all ones"-type, the delays are estimated by MUSIC according to

$$\hat{\chi} = \arg\max_{\chi} \frac{\|\hat{\mathbf{U}}^T(0)\mathbf{c}(\chi)\|^2}{\|\mathbf{c}(\chi)\|^2}, \tag{29}$$

where now $\hat{\mathbf{U}}(0)$ consists of N principal eigenvectors of $\hat{\mathbf{R}}(0)$. N is called the signal subspace dimension, which is equal to the rank of $\mathbf{G}$, see Eq. (8), or C at the

maximum. Here the columns of $\hat{\mathbf{U}}(0)$ are said to span the so called *signal subspace*, which is orthogonal to the *noise subspace* spanned by the rest eigenvectors of $\hat{\mathbf{R}}(0)$. Dimensions of the spaces are $\min\{N, C\}$ and $\max\{C - N, 0\}$, respectively. Considering the data model (3), N can be as high as $N = 2KL$ due to multipath fading, and even in non-fading case N is still as large as $N = 2K$. In highly loaded system, when $N > C$, $\hat{\mathbf{R}}(0)$ do not obey subspace structure anymore, and this causes the failure of MUSIC. In DC-MUSIC, on the other hand, the first thing to do is to filter interference and noise out as much as possible by differential correlations, i.e. by estimating $\hat{\mathbf{R}}(\tau)$ instead of $\hat{\mathbf{R}}(0)$. After this MUSIC is applied by estimating the L principal eigenvectors of symmetrized $\hat{\mathbf{R}}_{\text{sym}}(\tau)$.

TIMING-OFFSET ESTIMATION

Up to this point we have considered only coarse delay estimation by fractional testdelays, which is clearly enough to achieve an estimation error less that half a chip duration. The accurary of the estimate can then be achieved in tracking mode. Of course, accuracy could be achieved also by using smaller stepsizes for the testdelays. However, differential correlations enable actually solving the fractional part of the delay. Namely, we show in the following that in a frequency-flat fading channel it is enough to solve a system of two second-order polynomials for each chip interval.

Assume that only one resolvable path exists. Suppose $d+\delta$ is the propagation delay, so that the differential correlation matrix becomes $\mathbf{R}(\tau) = \bar{\alpha}(\tau)\mathbf{c}_{11}\mathbf{c}_{11}^T$. Recall that $\mathbf{c}_{11} = \underline{\mathbf{c}}_{11} + \overline{\mathbf{c}}_{11}$ by Eq. (20). According to Eqs. (4) and (5), we have moreover $\mathbf{c}_{11} = (1 - \delta)\mathbf{g}_1(d) + \delta\mathbf{g}_1(d + 1)$, where $\mathbf{g}_1(d)$ and $\mathbf{g}_1(d + 1)$ are defined in Eq. (24), being just a d and $d + 1$ times shifted replicas of the desired chip sequence, respectively. Suppose now that we use testcodes exatly $\mathbf{g}_1(d)$ and $\mathbf{g}_1(d+1)$. This is because the true delay lies between d and $d+1$. Considering the MF-type approach,

we immediately have (see details in the Appendix B)

$$|\mathbf{g}_1(d)^T\mathbf{R}(\tau)\mathbf{g}_1(d)| = |\bar{\alpha}(\tau)|[(1-\delta)\eta(0)+\delta\eta(1)]^2 \quad (30)$$

$$|\mathbf{g}_1(d+1)^T\mathbf{R}(\tau)\mathbf{g}_1(d+1)| = |\bar{\alpha}(\tau)|[(1-\delta)\eta(1)+\delta\eta(0)]^2, \quad (31)$$

where $\eta(i) \stackrel{\text{def}}{=} \mathbf{g}_1(d)^T\mathbf{g}_1(d+i)$. Notice that these quantities are known, since they are (up to scaling) just values of the code autocorrelation function with time lag i chips. For example, for m-sequences $\eta(0) = C$, and $\eta(1) = -1$. Hence, only two unknowns, $|\bar{\alpha}(\tau)|$ and δ are included in Eqs. (30) and (31). The solutions for δ can be found (see details in the Appendix C) to be equal to

$$\delta = \delta(d) = \frac{\eta(0) \mp P(d)\eta(1)}{(\eta(0)-\eta(1))(1 \pm P(d))}, \quad (32)$$

where

$$P(d) = \sqrt{\frac{|\mathbf{g}_1(d)^T\mathbf{R}(\tau)\mathbf{g}_1(d)|}{|\mathbf{g}_1(d+1)^T\mathbf{R}(\tau)\mathbf{g}_1(d+1)|}}. \quad (33)$$

Eq. (32), which we label ADC-MF (Accurate DC-MF), is a closed form expression for the timing offset δ, for which we need only the information about the hypotheses d and $d+1$. ADC-MF is summarized in Table 1.

Also MUSIC-type approach could be used. This is because $\mathbf{R}(\tau) = \bar{\alpha}(\tau)\mathbf{c}_{11}\mathbf{c}_{11}^T$ has only one non-zero eigenvalue, and the related eigenvector is $\mathbf{c}_{11}/\|\mathbf{c}_{11}\|$. Replacing $\mathbf{R}(\tau)$ by $\mathbf{U}(\tau)\mathbf{U}(\tau)^T = \mathbf{c}_{11}\mathbf{c}_{11}^T/\|\mathbf{c}_{11}\|^2$ is Eqs. (30) and (31), we would have

$$|\mathbf{g}_1(d)^T\mathbf{U}(\tau)\mathbf{U}(\tau)^T\mathbf{g}_1(d)| = \frac{1}{\|\mathbf{c}_{11}\|^2}[(1-\delta)\eta(0)+\delta\eta(1)]^2 \quad (34)$$

$$|\mathbf{g}_1(d+1)^T\mathbf{U}(\tau)\mathbf{U}(\tau)^T\mathbf{g}_1(d+1)| = \frac{1}{\|\mathbf{c}_{11}\|^2}[(1-\delta)\eta(1)+\delta\eta(0)]^2. \quad (35)$$

Since $\|\mathbf{c}_{11}\|$ is unknown, as being a function of δ, we end up with Eqs. (32) and (33). Naturarly, $\mathbf{R}(\tau)$ is replaced by $\mathbf{U}(\tau)\mathbf{U}(\tau)^T$ in Eq. (33). Analogously, we label this approach as ADC-MUSIC (Accurate DC-MUSIC), and summarize it also in Table 1.

Remark 4. A slightly modyfied version of Eq. (32) could be used also in case of multipaths. This is because now

$$\begin{aligned}\bar{\mathbf{R}}(\tau) &= \sum_{l=1}^{L} \bar{\alpha}_l(\tau)\mathbf{c}_{1l}\mathbf{c}_{1l}^T \text{ , i.e. Eq. (19)} \\ &= \sum_{l=1}^{L} \bar{\alpha}_l(\tau)[(1-\delta_l)^2\mathbf{g}_1(d_l)\mathbf{g}_1(d_l)^T \\ &+ 2\delta_l(1-\delta_l)\mathbf{g}_1(d_l)\mathbf{g}_1(d_l+1)^T + \delta_l^2\mathbf{g}_1(d_l+1)\mathbf{g}_1(d_l+1)^T]. \qquad (36)\end{aligned}$$

Letting now $d = d_1$, equations (30) and (31) would accordingly have more general forms

$$\begin{aligned}\mathbf{g}_1(d_1)^T\mathbf{R}(\tau)\mathbf{g}_1(d_1) &= \bar{\alpha}_1(\tau)[(1-\delta_1)\eta(0) + \delta\eta(1)]^2 \\ &+ \sum_{l=2}^{L} \bar{\alpha}_l(\tau)[(1-\delta_l)\eta(d_1-d_l) + \delta\eta(d_1-d_l-1)]^2 \qquad (37) \\ \mathbf{g}_1(d_1+1)^T\mathbf{R}(\tau)\mathbf{g}_1(d_1+1) &= \bar{\alpha}_1(\tau)[(1-\delta)\eta(1) + \delta\eta(0)]^2 \\ &+ \sum_{l=2}^{L} \bar{\alpha}_l(\tau)[(1-\delta_l)\eta(d_1-d_l-1) + \delta\eta(d_1-d_l)]^2 \qquad (38)\end{aligned}$$

Assuming impulse-like code autocorrelation, i.e. $\eta(i) \approx 0$ for $|i| \geq 1$, we would end up with (30) and (31), where in addition $\eta(1) = 0$. This would accordingly lead to an estimator

$$\hat{\delta} = \frac{1}{1 \pm P(d)}. \qquad (39)$$

3. NUMERICAL EXPERIMENTS

We compared the methods in the downlink environment with Rayleigh fading channel. Data rate was assumed to be $f_d = 16$ kbit/s, carrier frequency $f_c = 1.8$ GHz, and mobile speed $v = 50$ km/h. This results in normalized Doppler shifts at most $\frac{v}{v_{\text{light}}} f_c/f_d = 5.21 \cdot 10^{-3}$. Typical fading process at the symbol level is seen in Figure 3.

The delays were estimated in parallel manner, and the strongest peak from the delay sprectum was selected. Acquisition was declared if this peak corresponded to the

strongest path. Hence, our requirement is more stringent than the other common definition, for which it is sufficient just to find any multipath component. The measured performance parameters were probability of acquisition, mean acquisition time, and root-mean-square-error (RMSE). Mean acquisition time (in symbols) was measured as [23]

$$T_{ACQ} = \frac{MC + T_P(1 - Pr_{ACQ})}{Pr_{ACQ}} T_c, \tag{40}$$

where T_P and T_c are the penalty time, in case of misacquisition and chip duration, respectively. In our simulations we had $T_P = 500$ symbols and $T_c = \frac{1}{C} = \frac{1}{31}$ symbols. Pr_{ACQ} is the probability of acquisition. The other performance parameter, RMSE, measures the accuracy of the delay estimate according to

$$\text{RMSE} = \sqrt{\frac{1}{S}\sum_{i=1}^{S}(\hat{d}_i - d)^2}, \tag{41}$$

where S is the number of simulations.

The methods for delay estimation were: DC-MF (23), DC-MUSIC (28), ADC-MF and ADC-MUSIC (Table 1), MUSIC (29), CMOE [17] , and conventional non-coherent and coherent MF [4]. Any parameters such as time-varying path strengths, and codes of the interfering users were not assumed to be known. Only the code of the desired user was known. In addition, a preamble $b_{1m} = 1$ was available for the desired user $k = 1$. Gold codes of length $C = 31$ were used. Signal-to-Noise Ratio (SNR) in the chip-matched filter output was always 10 dB. In frequency-selective fading channel the number of paths was $L = 3$ if not otherwise stated. Relative differences in paths powers were 5 dB, and SNR was always set with respect to the strongest path. The number of users K was varied from $K = 5$ to $K = 25$. Therefore, the total number of sources was $2KL = 6K = 30, \ldots 150$, while the maximum signal subspace dimension was $C = 31$. Therefore, highly loaded systems arise. We noticed that the performance of MUSIC became better by selecting the estimated signal subspace dimension $2K$ instead of $2KL$. This can be justified also

by the fact that usually it is impossible to know the number of paths, while number of users can be known by uplink-downlink communication. In one simulation, each parameter value was fixed, and the delays were estimated from the peaks of the delay spectra. All the measured quantitites are averaged over 1000 simulations.

In the first experiment we studied the effect of increasing the length of the preamble. The system included $K = 20$ users and the desired user had either equal or 5 dB weaker signal power than the others. From Figure 4 we see that non-coherent MF failed in near-far scenario, which was predictable, as well as MUSIC due to high system load. The zero mean fading process also seemed to be too fast for the coherent MF, even though it was in this setting the most robust against MAI. CMOE performed better the more samples were available. This was because the estimate for the inverse of the autocorrelation matrix $\mathbf{R}(0)$ thus became more accurate. However, in the presence of MAI, see Figure 5, CMOE did not really managed to catch at least the strongest path first. The fact that the proposed methods are asymptotically invariant with respect to the interfering users and noise can be predicted from Figures 4 and 5, in which the probability of acquisition seems to tend to the to 1, whether the MAI is 0 or 5. In this experiment, $M = 500$ symbols were enough for them to achieve almost the same performance whether the interfering users were 5 dB stronger or not. The figures also tell the fact that the performance of the proposed methods depends essentially on the lenght of the preamble, because the goal is to average interference out. For this reason, it is clear that the methods fail if the preamble is too short. On the other hand, although coherent MF was the best among the others when short preamble is used, its performance remained at moderate level. In Figures 6 and 7, the mean acquisition times in symbols are plotted. Due to the reliable estimation, the acquisition time for the proposed methods was usually no more than the length of the preamble. As can be seen from Figure 5, coherent MF was in average the fastest if only a short preamble was available. One

can also notice, that DC-MF seemed to have better acquisition cabability of the strongest path than DC-MUSIC. The reason for this is that MF-type approaches work in general well as the code autocorrelation function is impulse-like. To show the power of DC-MUSIC when the code autocorrelation is not that spiky, we assigned $K = 2$ users random codes of lenght $C = 7$ in $L = 3$ path Rayleigh fading channel. The paths had 5 dB differences in power. Figure 8 shows the average number of acquired paths as a function of preamble length. It is seen that already with preamble lenght $M = 100$ DC-MUSIC found the most of the paths. Table 2 shows the case $M = 500$ in more detail. Namely, it tells the number of cases when each path was acquired. It is quite noticeable how frequently DC-MUSIC acquired also the weaker paths (-5 dB and -10 dB paths with probabilities 0.917 and 0.629, respectively) compared to the other methods, which had serious problems in acquiring even the second strongest path.

In the second experiment we studied the effect of system loading, i.e. when the number of users was increased. The system included $K = 5$ to $K = 25$ users with MAI equal to 0 dB. The length of the preamble was $M = 500$ symbols. Figure 9 shows the achieved probability of acquisition. Although the true model order (equal to $2KL$) was quite high, the model order underestimation (estimated as $2K$) helped MUSIC in the case of $K = 5$ users. This was not the case for the other system loads. Coherent MF had nearly the same performance regardless of the system load, althoug the performance level again was moderate. The difference of the other remaining methods (DC-MF,DC-MUSIC,CMOE, and MF) in this experiment was too small up to $K = 15$ users to draw conclusions. This was mainly because of the MAI free case. On the other hand, especially in the case $K = 25$, which means quite a heavy system load, the proposed methods clearly performed the best. It is also seen that coherent MF, together with the proposed methods are the most robust against system loading. But among those only the proposed ones can exploit the

time-correlatedness of the fading process, resulting with better performance level. Figure 10 tells the corresponding mean acquisition times. Assuming the bit rate of 16 kbit/s, these times for the case $K = 25$ would equal the following: DC-MF and DC-MUSIC 33 ms, coherent MF 44 ms, CMOE 52 ms, and non-coherent MF 54 ms. Thus, at least 25% improvement would be gained by the proposed methods, compared to any reference ones.

In the third experiment we studied the behavior of the methods when increasing the number of inter-symbol-interference (ISI). The ISI was generated by increasing the number of paths from $L = 2$ to $L = 10$. One of the paths was always 5 dB stronger, which was intended to be acquired. System included $K = 20$ users, and $M = 500$ symbols were used again as a preamble. MUSIC was no more applied due to its obvious failure in highly loaded systems (see the first experiment). Hence, the only method which would need to know or estimate the number of paths L, is DC-MUSIC. Recall that DC-MUSIC computes L eigenvectors. In this experiment DC-MUSIC always assumed $L = 3$. Figure 11 shows that proposed methods clearly resist ISI the best. Moreover, DC-MUSIC seems not to be that sensitive to the model order mismatch.

In the fourth experiment, we studied the achieved accuracy in a system with $K = 20$ users. Although MUSIC is a high-resolution method, it was not applied, again, due to its failure in this setting. The channel was frequency-flat fading, and ADC-MF and ADC-MUSIC were applied for the first time. The accuracy for all the other methods was achieved by using more delay candidates. More precisely, the increment for the delay candidate was always as small as $\frac{1}{100}$ chip. Recall that ADC-MF and ADC-MUSIC uses an increment equal to one chip, only. Figure 12 shows the achieved accuracies in RMSE. It can be stated that the high-resolution feature of MUSIC is now seen in the performance of ADC-MUSIC, which reached an RMSE

of only $0.02 - 0.04$ chips, depending on the system load. CMOE seems also to yield quite accurate estimates, and performs better than ADC-MF, which reached RMSE of $0.04 - 0.08$ chips. However, it must be pointed out that there was no MAI in this experiment. It is hence expected that in the presence of MAI, the RMSE of CMOE as well as coherent and non-coherent MF will degrade significantly, as did in the first experiment.

The final experiment was dedicated for the comparison of the accuracy of ADC-MF and ADC-MUSIC to the Cramer-Rao lower bound (CRB). Although the estimators turned out to be approximately unbiased, the bias was estimated for each fixed parameter value. This was taken into account in the final RMSE calculation, giving an adequate measure for CRB comparison. The system included $K = 5$ users, and the average SNR was 10 dB. Single-path time-invariant channel was assumed, and hence the data model coincide e.g. that of [10], where the CRB was derived [pp. 88-89]. The RMSE curves are seen in Figure 13, from which we notice that neither methods attain the CRB. This was the case also in [9] with MUSIC. However, it must be pointed out that the preamble is not yet optimally utilized in ADC-MF nor in ADC-MUSIC. This is because the contribution of interference and noise was tried to suppress by estimating only one differential correlation matrix $\hat{\mathbf{R}}(\tau)$, with $\tau = 2$ in all the experiments. But especially with slowly fading channels, strong time correlatations takes place with much larger time intervals, which suggests the possibility of achieving even more interference suppression, and consequently better accuracy.

DERIVATION OF EQUATION (19)

First, from Eq. (8) we have

$$\mathbf{GA}(\tau) = [\underline{\mathbf{c}}_{11}, \overline{\mathbf{c}}_{11}, \ldots, \underline{\mathbf{c}}_{1L}, \overline{\mathbf{c}}_{1L}, \ldots, \underline{\mathbf{c}}_{KL}, \overline{\mathbf{c}}_{KL}] \left[\begin{array}{ccc|c} \mu_1^2\bar{\alpha}_1(\tau)\mathbf{1} & & \mathbf{0} & \\ & \ddots & & \mathbf{0} \\ \mathbf{0} & & \mu_L^2\bar{\alpha}_L(\tau)\mathbf{1} & \\ \hline & \mathbf{0} & & \mathbf{0} \end{array}\right] \quad (42)$$

$$= [\mu_1^2\bar{\alpha}_1(\tau)(\underline{\mathbf{c}}_{11} + \overline{\mathbf{c}}_{11}) \cdots \mu_L^2\bar{\alpha}_L(\tau)(\underline{\mathbf{c}}_{1L} + \overline{\mathbf{c}}_{1L})\ 0 \cdots 0] \quad (43)$$

$$= [\mu_1^2\bar{\alpha}_1(\tau)\mathbf{c}_{11} \cdots \mu_L^2\bar{\alpha}_L(\tau)\mathbf{c}_{1L}\ 0 \cdots 0], \quad (44)$$

where the second equation follows from $\mathbf{1} = \begin{bmatrix} 1 & 1 \\ 1 & 1 \end{bmatrix}$, and the third is due to definition $\mathbf{c}_{1l} = \underline{\mathbf{c}}_{1l} + \overline{\mathbf{c}}_{1l}$. Therefore we have

$$\mathbf{GA}(\tau)\mathbf{G}^T = \sum_{l=1}^{L} \mu_l^2\bar{\alpha}_l(\tau)(\mathbf{c}_{1l}\underline{\mathbf{c}}_{1l}^T + \mathbf{c}_{1l}\overline{\mathbf{c}}_{1l}^T), \quad (45)$$

from which (19) immediately follows.

DERIVATION OF EQUATIONS (30) AND (31)

Recall from section 3.3, that

$$\mathbf{R}(\tau) = \bar{\alpha}(\tau)\mathbf{c}_{11}\mathbf{c}_{11}^T \text{ , and} \quad (46)$$

$$\mathbf{c}_{11} = (1-\delta)\mathbf{g}_1(d) + \delta\mathbf{g}_1(d+1). \quad (47)$$

Thus, we first may write

$$\begin{aligned} \mathbf{c}_{11}\mathbf{c}_{11}^T &= (1-\delta)^2\mathbf{g}_1(d)\mathbf{g}_1(d)^T + \delta^2\mathbf{g}_1(d+1)\mathbf{g}_1(d+1)^T \\ &+ \delta(1-\delta)\mathbf{g}_1(d)\mathbf{g}_1(d+1)^T + \delta(1-\delta)\mathbf{g}_1(d+1)\mathbf{g}_1(d)^T. \end{aligned} \quad (48)$$

Defining $\eta(i) = \mathbf{g}_1(d)^T\mathbf{g}_1(d+i)$, we have

$$\begin{aligned} \mathbf{g}_1(d)^T\mathbf{R}(\tau)\mathbf{g}_1(d) &= \bar{\alpha}(\tau)[1-\delta)^2\eta(0)^2 + \delta^2\eta(1)^2 + \delta(1-\delta)\eta(0)\eta(1) + \delta(1-\delta)\eta(1)\eta(0)] \\ &= \bar{\alpha}(\tau)[(1-\delta)\eta(0) + \delta\eta(1)]^2, \end{aligned} \quad (49)$$

from which Eq. (30) follows. The derivation of Eq. (31) is entirely similar and is omitted.

DERIVATION OF EQUATION (32)

To shorten notations, define $A = \mathbf{g}_1(d)^T\mathbf{R}(\tau)\mathbf{g}_1(d)$ and $B = \mathbf{g}_1(d+1)^T\mathbf{R}(\tau)\mathbf{g}_1(d+1)$. Taking squareroots on both sides of Eqs. (30) and (31), we have

$$\pm\sqrt{A} = \sqrt{\bar{\alpha}(\tau)}[(1-\delta)\eta(0) + \delta\eta(1)] \quad (50)$$

$$\pm\sqrt{B} = \sqrt{\bar{\alpha}(\tau)}[(1-\delta)\eta(1) + \delta\eta(0)], \quad (51)$$

which is a system of equations with two unknowns, δ, and $\sqrt{\bar{\alpha}(\tau)}$. Dividing Eq. (50) by Eq. (51) we obtain

$$\pm\sqrt{\frac{A}{B}} = \frac{(1-\delta)\eta(0) + \delta\eta(1)}{(1-\delta)\eta(1) + \delta\eta(0)}. \quad (52)$$

By simple algebraic manipulations it leads to

$$\delta[\pm\sqrt{\frac{A}{B}}\eta(0) \mp \sqrt{\frac{A}{B}}\eta(1) + \eta(0) - \eta(1)] = \eta(0) \mp \sqrt{\frac{A}{B}}\eta(1), \quad (53)$$

from which Eq. (32) is obtained by denoting $P(d) = \sqrt{\frac{A}{B}}$.

According to a further aspect of the invention, a synchronization method in a spread spectrum receiver is provided, in which method matched filtering is employed and the delay of received signal is estimated. In an advantageous embodiment of the invention, in matched filtering, a set of test delays is scanned through with the pseudonoise code used in matched filtering, consecutive test delays having a delay difference of one chip interval, and each different test delay producing a sequence of matched filtering results, and

each said sequence of matched filtering results is correlated with a delayed copy of each said sequence of matched filtering results for producing a correlation result value corresponding to the test delay producing said sequence of matched filtering results,

and in that, that delay estimation comprises steps, in which

- two further test delays are calculated from each pair of two consecutive correlation result values,
- it is checked for each of said two further test delays, if the test delay is between the test delay values corresponding to said pair of two consecutive correlation result values, and if it is, the test delay is added to the set of test delays, and
- a delay from the set of test delays is selected to be a result of delay estimation.

In the step of calculation of two further test delays, preferably equation (32) or equation (39) is used.

The present aspect of the invention is illustrated further in figure 14, which shows a part of a block diagram of a spread spectrum receiver. Figure 14 shows a matched filter block 10, a delay block 15, a correlation block 20, and a delay estimation block 30. In the figure, r(t) denotes the stream of sample vectors, and PN denotes the pseudonoise i.e. code fed into the matched filter block 10. Different matched filtering results are obtained using a set of test delay values for the pseudonoise code PN fed into the matched filtering block, and each stream of matched filtering results is correlated with a delayed copy of itself for producing a correlation result value. In the delay estimation block, further test delays are calculated on the basis of said correlation result values, and the test delay producing the best match to the received samples is selected as the estimated delay. It is also possible to select a plurality of the test delays, if the signal from more than one paths is desired to be detected.

The selection of a test delay to be a result of the delay estimation can advantageously be performed using condition (26).

In one advantageous embodiment of the invention, more than one delays are estimated. In such an embodiment, after the first test delay is selected as a result of the estimation, the test delay is removed from the set of test delays as well as all those test delays, whose delay difference to the selected and removed test delay is less than one chip interval. The next delay estimate is then selected from the remaining set.

According to a further aspect of the invention, a synchronization method in a spread spectrum receiver is provided, in which method signal subspace estimation is employed. According to an advantageous embodiment of the invention, sampled data and at least one delayed version of sampled data is used in the signal subspace estimation in the method, and the method further comprises the step of calculation of a signal subspace which is substantially the same as a signal subspace calculated of a combination of at least two matrices, which matrices have the form of $\mathbf{M}\mathbf{M}_n^H$, where $\mathbf{M}$ is a matrix composed of a first set of data samples, and $\mathbf{M}_n^H$ is the hermitian transpose of a matrix composed of a second set of data samples, said second set of data samples having a time difference of n sampling intervals to samples of said first set of data samples.

The time difference n can be a positive or a negative integer, whereby the second set of data samples may be an earlier set or a later set as the first set of data samples. We note here that with small values of n, i.e. when the absolute value of n is smaller than the size of the sets of data samples forming the matrices $\mathbf{M}$ and $\mathbf{M}_n$, the matrices may have some overlap. In other words, the matrices $\mathbf{M}$ and $\mathbf{M}_n$ are formed of sample vectors $\mathbf{r}_a \ldots \mathbf{r}_m$ and $\mathbf{r}_{a+n} \ldots \mathbf{r}_{m+n}$, respectively, where $\mathbf{r}_a$ is the first sample vector in $\mathbf{M}$ and $\mathbf{r}_m$ the last sample vector in $\mathbf{M}$.

In various embodiments of the invention, the signal subspace can be calculated in many different ways, for example directly from the data vectors. The signal subspace can also be calculated from the combination of $\mathbf{M}\mathbf{M}_n^H$ matrix products. In a further advantageous embodiment of the invention, in the step of calculation of a signal subspace, said signal subspace is calculated of a combination of at least two matrices, which matrices have the form of $\mathbf{M}\mathbf{M}_n^H$, where $\mathbf{M}$ is a matrix composed of a first set of data samples, and $\mathbf{M}_n^H$ is the hermitian transpose of a matrix composed of a second set of data samples, said second set of data samples having a time difference of n sampling intervals to samples of said first set of data samples.

Said combination is preferably a linear combination, which is useful for symmetrization purposes. However, the invention is in no way limited only to a linear combination of matrices of the form of $\mathbf{MM}_n^H$.

Calculation of a signal subspace of matrix A refers to the calculation of such a subspace, whose basis vectors span the same subspace as the eigenvectors of matrix A corresponding to the largest eigenvalues of matrix A. Calculation of signal subspace is in itself well known to a man skilled in the art, wherefore it is not described in more detail in this application.

The present aspect of the invention is illustrated further in figure 15. The figure shows a part of the block diagram of a spread spectrum receiver. Figure 15 shows a signal subspace estimation block 60, whose function is to produce an estimate of the signal subspace for use in delay estimation. According to the invention, delayed sample matrices are used the signal subspace estimation in addition to sample matrices collected without delay. This is represented by delay blocks 50 in figure 15. As the figure illustrates, there may be more than one delay, which is to say that the signal subspace estimation can be performed on the basis of a plurality of products $\mathbf{MM}_n^H$, where each delay corresponds to a different value of n. As stated before, the length of the delay is an integer multiple of the sampling interval. In the figure, r(t) denotes the stream of sample vectors.

According to an advantageous embodiment of the invention, a synchronization methods according to an advantageous embodiment of the invention is used in a mobile communication means of a cellular telecommunication system.

In an advantageous embodiment of the invention, a mobile communication means is provided, which mobile communication means comprises

- a subspace estimation block arranged to use sampled data and at least one delayed version of sampled data is used in the signal subspace estimation, and
- means for calculation of a signal subspace which is substantially the same as a signal subspace calculated of a combination of at least two matrices,

which matrices have the form of $\mathbf{MM}_n^H$,

where $\mathbf{M}$ is a matrix composed of a first set of data samples, and $\mathbf{M}_n^H$ is the hermitian transpose of a matrix composed of a second set of data samples, said second set of data samples having a time difference of n sampling intervals to samples of said first set of data samples.

According to an advantageous embodiment of the invention, a synchronization methods according to an advantageous embodiment of the invention is used in used in a global positioning system (GPS) receiver.

In an advantageous embodiment of the invention, global positioning system receiver is provided, which receiver comprises
- a subspace estimation block arranged to use sampled data and at least one delayed version of sampled data is used in the signal subspace estimation, and
- means for calculation of a signal subspace which is substantially the same as a signal subspace calculated of a combination of at least two matrices,
which matrices have the form of $\mathbf{M}\mathbf{M}_n^H$,
where $\mathbf{M}$ is a matrix composed of a first set of data samples, and $\mathbf{M}_n^H$ is the hermitian transpose of a matrix composed of a second set of data samples, said second set of data samples having a time difference of n sampling intervals to samples of said first set of data samples.

According to an advantageous embodiment of the invention, a synchronization methods according to an advantageous embodiment of the invention is used in a receiver of a wireless local area network (WLAN) terminal.

In an advantageous embodiment of the invention, a terminal of a wireless local area network is provided, which terminal comprises
- a subspace estimation block arranged to use sampled data and at least one delayed version of sampled data is used in the signal subspace estimation, and
- means for calculation of a signal subspace which is substantially the same as a signal subspace calculated of a combination of at least two matrices,
which matrices have the form of $\mathbf{M}\mathbf{M}_n^H$,
where $\mathbf{M}$ is a matrix composed of a first set of data samples, and $\mathbf{M}_n^H$ is the hermitian transpose of a matrix composed of a second set of data samples, said second set of data samples having a time difference of n sampling intervals to samples of said first set of data samples.

According to an advantageous embodiment of the invention, the synchronization methods according to various embodiments of the invention are used in radio link receivers employing spread spectrum technology. For example, any synchronization method described in this specification can be used for example in the well-known Bluetooth device.

The present invention provides an improved method for performing initial synchronization. The invention can be used with any tracking mechanisms and other mechanisms associated with spread spectrum reception, wherefore the invention is not limited to to being used with any specific tracking mechanisms or other mechanisms associated with spread spectrum reception.

The equations described in this specification are meant to be examples only, since the same underlying ideas can be expressed in a multitude of different ways using different mathematical phraseology, as a man skilled in the art very well knows and understands. Therefore the invention is not limited to exactly those equations described in this specification nor to any other specific set of equations.

The inventive method is applicable in spread spectrum receivers. Practical examples of such applications which are commercially important at the time of writing this patent application are mobile stations of WCDMA cellular systems such as the UMTS, IS-95, and IMT-2000 cellular systems, global positioning system (GPS) receivers and wireless local area network (WLAN) terminals.

In view of the foregoing description it will be evident to a person skilled in the art that various modifications may be made within the scope of the invention. While a preferred embodiment of the invention has been described in detail, it should be apparent that many modifications and variations thereto are possible, all of which fall within the true spirit and scope of the invention.

Denote Ω the set of delay candidates.

1. Estimate the differential correlation matrix with time lag τ from available vector samples as $\hat{\mathbf{R}}(\tau) = \frac{1}{M}\sum_{m=1}^{M} \mathbf{r}_m \mathbf{r}_{m+\tau}^H$.

2. Let $\hat{\mathbf{U}}(\tau)$ contain L principal eigenvectors of $\hat{\mathbf{R}}(\tau) + \hat{\mathbf{R}}(\tau)^H$, where L is the number of paths to be acquired.

3. Set $\Omega = \{0, 1, \ldots, C\}$, i.e. multiples of a chip duration.

4. For each $d \in \Omega - \{C\}$ do:

   (a) Compute two candidates for fractional part of the delay, $\hat{\delta}(d)$, according to Eqs. (32) and (33). In the latter equation, replace

   - $\mathbf{R}(\tau)$ by $\hat{\mathbf{R}}(\tau)$ in case of ADC-MF,
   - $\mathbf{R}(\tau)$ by $\hat{\mathbf{U}}(\tau)\hat{\mathbf{U}}(\tau)^T$ in case of ADC-MUSIC

   (b) Insert $d + \hat{\delta}(d)$ to Ω, if $\hat{\delta}(d) \in (0, 1)$.

5. Obtain one delay estimate by choosing the strongest peak from the delay spectrum

$$\frac{|\mathbf{c}_1(\chi)^T \Theta \mathbf{c}_1(\chi)|}{\|\mathbf{c}_1(\chi)\|^2} \begin{cases} \Theta = \hat{\mathbf{R}}(\tau), \text{ ADC-MF} \\ \Theta = \hat{\mathbf{U}}(\tau)\hat{\mathbf{U}}(\tau)^T, \text{ ADC-MUSIC} \end{cases} \tag{54}$$

   where $\mathbf{c}_1(\chi)$ is a testcode of form Eq. (24), corresponding to delay $\chi \in \Omega$.

6. If other paths are acquired, too, choose such a next strongest peak of Eq. (54), which does not correspond to a delay closer than one chip to any already found delays.

Table 1: Algorithms ADC-MF and ADC-MUSIC for timing offset estimation.

path	1st	2nd	3rd	
power	0 dB	−5 dB	−10 dB	
delay (chips)	$1+\delta_1$	$3+\delta_2$	$5+\delta_3$	
	#/1000	#/1000	#/1000	Σ/3000
DC-MUSIC	969	917	629	2515
DC-MF	975	710	414	2099
MF	958	620	357	1935
coh. MF	878	570	404	1851
CMOE	953	765	433	2151

Table 2: Number of cases a certain path was acquired in a $K = 2$ user system with random codes of length $C = 7$. Preamble length was $M = 500$ symbols, and average SNR was 10 dB. The fractional parts δ_i, $i = 1, 2, 3$ were uniformly distributed over $(0, 1)$.

REFERENCES

[1] T. Ojanperä, and R. Prasad, *Wideband CDMA for Third Generation Mobile Communications*, Artech House, 1998.

[2] H.V. Poor, "On parameter estimation in DS/CDMA formats", in *Advances in Communications and Signal Processing*, W.A. Porter and S.C. Kak, Eds., New York: Springer-Verlag, 1989.

[3] K.K. Chawla, and D.C. Sarwate, "Parallel Acquisition of PN Sequences in DS/SS Systems", *IEEE Transactions on Communications*, vol. 42, pp. 2155-2164, May 1994.

[4] J.G. Proakis, *Digital Communications*, third edition, McGraw-Hill, 1995.

[5] S. Verdú, "Minimum Probability of Error for Asynchronous Gaussian Multiple-Access Channels", *IEEE Transactions on Information Theory*, vol. 32, no. 1, January 1986, pp. 85-96.

[6] R. Lupas, S. Verdú, "Linear multiuser detectors for synchronous code-division multiple-access communications", *IEEE Trans. Inform. Theory*, vol. IT-35, pp. 123-136, January 1989.

[7] U. Madhow, and M.L. Honig, "MMSE Interference Suppression for Direct-Sequence Spread-Spectrum CDMA", *IEEE Transactions on Communications*, vol. 42, no. 12, pp. 3178-3188, December 1994.

[8] S. Bensley and B. Aazhang, "Subspace-Based Channel Estimation for Code Division Multiple Access Communication Systems". *IEEE Transactions on Communications*, vol. 44, no. 8, August 1996, pp. 1009-1020.

[9] E. Ström, S. Parkvall, S. Miller, and B. Ottersten, "Propagation Delay Estimation in Asynchronous Direct-Sequence Code Division Multiple Access Systems", *IEEE Transactions on Communications*, vol. 44, January 1996, pp. 84-93.

[10] D. Zheng, J. Li, S.L. Miller, and E.G. Ström, "An efficient code-timing estimator for DS-CDMA signals", *IEEE Trans. Sign. Proc.*, vol. 45, no. 1, pp. 82-89, Jan. 1997.

[11] S.E. Bensley and B. Aazhang, "Maximum Likelihood Synchronization of a Single User for Code Division Multiple Access Communication Systems," *IEEE Trans. Communications*, vol. 46, no. 3, March 1998, pp. 392-399.

[12] R. Schmidt, "Multiple Emitter Location and Signal Parameter Estimation", *IEEE Transactions on Antennas and Propagation*, AP-34, March 1986, pp. 276-290.

[13] Z.-S. Liu, J. Li, and S.L. Miller, "An Efficient Code-Timing Estimator for Receiver Diversity DS-CDMA Systems", *IEEE Transactions on Communications*, vol. 46, no. 6, pp. 826-835, June 1998.

[14] M.H. Zarrabizadeh and E.S. Sousa, "A Differentially Coherent PN Code Acquisition Receiver for CDMA Systems", *IEEE Transactions on Communications*, vol. 45, no. 11, pp. 1456-1465, November 1997.

[15] C.-D. Chung, "Differentially Coherent Detection Technique for Direct-Sequence Code Acquisition in a Rayleigh Fading Channel", *IEEE Transactions on Communications*, vol. 43, no. 2/3/4, pp. 1116-1126, February/March/April 1995.

[16] S. Parkvall, *Near-Far Resistant DS-CDMA Systems: Parameter Estimation and Data Detection.* Ph.D. Thesis, Royal Institute of Technology, October 1996.

[17] M. Latva-Aho, "Advanced Receivers for Wideband CDMA Systems", Doctoral Thesis, Acta. Univ. Ouluensis, C 125, September 1998.

[18] J.D. Parsons, *The Mobile Radio Propagation Channel*, Pentech Press, London, 1992.

[19] J. Joutsensalo and T. Ristaniemi, "Single-User Synchronization in Fading Channel", in *Proc. IEEE Signal Processing Workshop on Signal Processing*

Advances in Wireless Communications, Annapolis, Maryland, USA, May 9-12, 1999, pp. 133-137.

[20] M.L. Honig, U. Madhow, and S. Verdu, "Blind Adaptive Multiuser Detection," *IEEE Trans. Information Theory*, vol. 41, no. 4, pp. 944-960, July 1995.

[21] U. Madhow, "Blind adaptive interference suppression for direct-sequence CDMA" , *Proc. IEEE*, October 1998.

[22] M. Latva-Aho, J. Lilleberg, J. Iinatti, and M. Juntti, "CDMA Downlink Code Acquisition Performance in Frequency-Selective Fading Channels", PIMRC'98, Boston, USA, September 8-11, 1998.

[23] A. Polydoros and C. Weber, "A unified approach to serial search spread-spectrum code acquisition - part II: A matched filter receiver", *IEEE Trans. Comm.*, vol. 32, no. 5, pp. 550-560, 1984.

Claims

1. Synchronization method in a spread spectrum receiver in which method signal subspace estimation is employed, **characterized** in that
sampled data and at least one delayed version of sampled data is used in the signal subspace estimation, and in that, that the method further comprises the step of calculation of a signal subspace which is substantially the same as a signal subspace calculated of a combination of at least two matrices,
which matrices have the form of $\mathbf{M}\mathbf{M}_n^H$,
where $\mathbf{M}$ is a matrix composed of a first set of data samples, and $\mathbf{M}_n^H$ is the hermitian transpose of a matrix composed of a second set of data samples, said second set of data samples having a time difference of n sampling intervals to samples of said first set of data samples.

2. A synchronization method according to claim 1, **characterized** in that
in the step of calculation of a signal subspace, said signal subspace is calculated of a combination of at least two matrices,
which matrices have the form of $\mathbf{M}\mathbf{M}_n^H$,
where $\mathbf{M}$ is a matrix composed of a first set of data samples, and $\mathbf{M}_n^H$ is the hermitian transpose of a matrix composed of a second set of data samples, said second set of data samples having a time difference of n sampling intervals to samples of said first set of data samples.

3. Synchronization method in a spread spectrum receiver in which method matched filtering is employed and the delay of received signal is estimated, **characterized** in that in the method,
in matched filtering, a set of test delays is scanned through with the pseudonoise code used in matched filtering, consecutive test delays having a delay difference of one chip interval, and each different test delay producing a sequence of matched filtering results, and
each said sequence of matched filtering results is correlated with a delayed copy of each said sequence of matched filtering results for producing a correlation result value corresponding to the test delay producing said sequence of matched filtering results,
and in that, that delay estimation comprises steps, in which
- two further test delays are calculated from each pair of two consecutive correlation result values,

- it is checked for each of said two further test delays, if the test delay is between the test delay values corresponding to said pair of two consecutive correlation result values, and if it is, the test delay is added to the set of test delays, and
- a delay from the set of test delays is selected to be a result of delay estimation.

4. A mobile station of a cellular telecommunication system utilizing spread spectrum communication,
characterized in that it comprises
- a subspace estimation block arranged to use sampled data and at least one delayed version of sampled data is used in the signal subspace estimation, and
- means for calculation of a signal subspace which is substantially the same as a signal subspace calculated of a combination of at least two matrices,
which matrices have the form of $\mathbf{M}\mathbf{M}_n^H$,
where $\mathbf{M}$ is a matrix composed of a first set of data samples, and $\mathbf{M}_n^H$ is the hermitian transpose of a matrix composed of a second set of data samples, said second set of data samples having a time difference of n sampling intervals to samples of said first set of data samples.

5. A global positioning system receiver,
characterized in that it comprises
- a subspace estimation block arranged to use sampled data and at least one delayed version of sampled data is used in the signal subspace estimation, and
- means for calculation of a signal subspace which is substantially the same as a signal subspace calculated of a combination of at least two matrices,
which matrices have the form of $\mathbf{M}\mathbf{M}_n^H$,
where $\mathbf{M}$ is a matrix composed of a first set of data samples, and $\mathbf{M}_n^H$ is the hermitian transpose of a matrix composed of a second set of data samples, said second set of data samples having a time difference of n sampling intervals to samples of said first set of data samples.

6. A terminal of a wireless data communications network,
characterized in that it comprises
- a subspace estimation block arranged to use sampled data and at least one delayed version of sampled data is used in the signal subspace estimation, and
- means for calculation of a signal subspace which is substantially the same as a signal subspace calculated of a combination of at least two matrices,
which matrices have the form of $\mathbf{M}\mathbf{M}_n^H$,
where $\mathbf{M}$ is a matrix composed of a first set of data samples, and $\mathbf{M}_n^H$ is the hermitian transpose of a matrix composed of a second set of data samples, said second set of data samples having a time difference of n sampling intervals to samples of said first set of data samples.

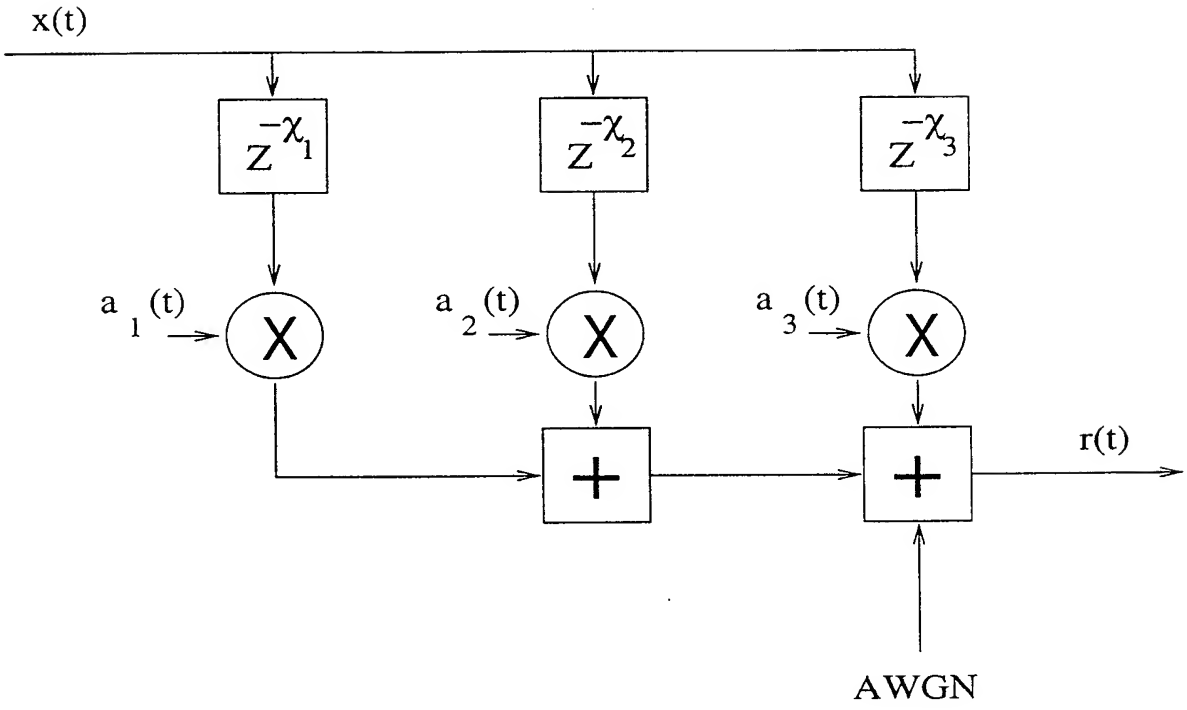

Fig. 1

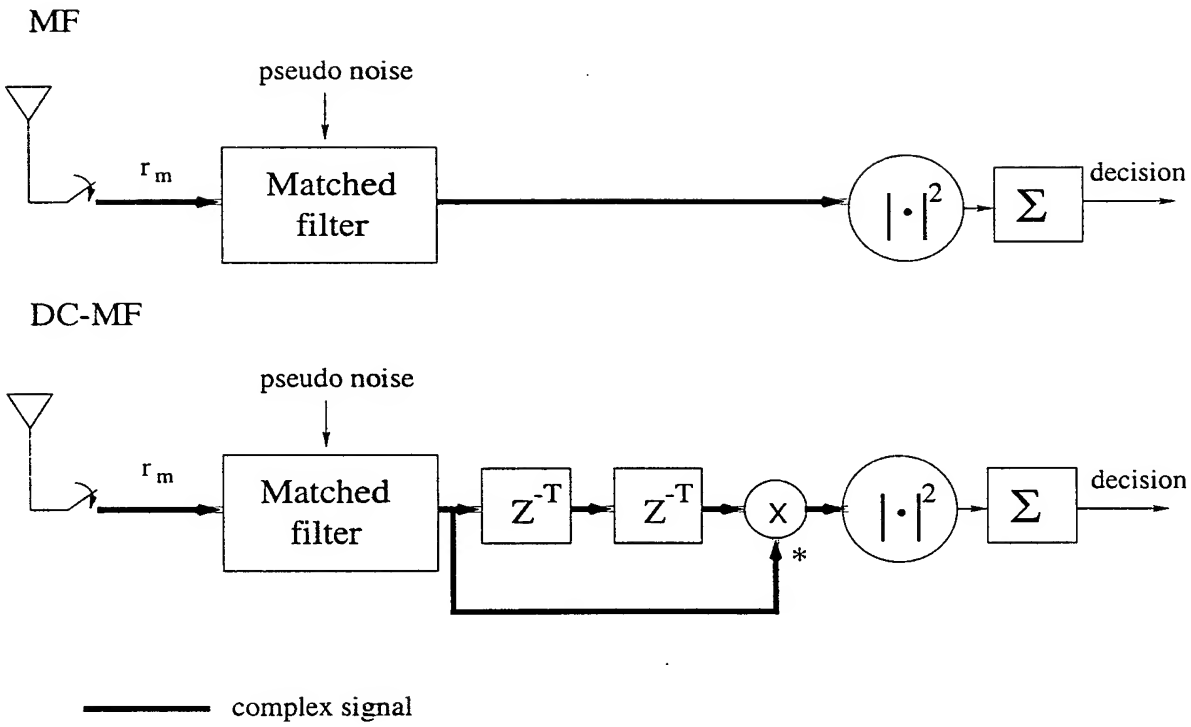
MF
pseudo noise
r_m
Matched filter
$|\cdot|^2$
Σ
decision
DC-MF
pseudo noise
r_m
Matched filter
Z^{-T}
Z^{-T}
X
*
$|\cdot|^2$
Σ
decision
complex signal

Fig. 2

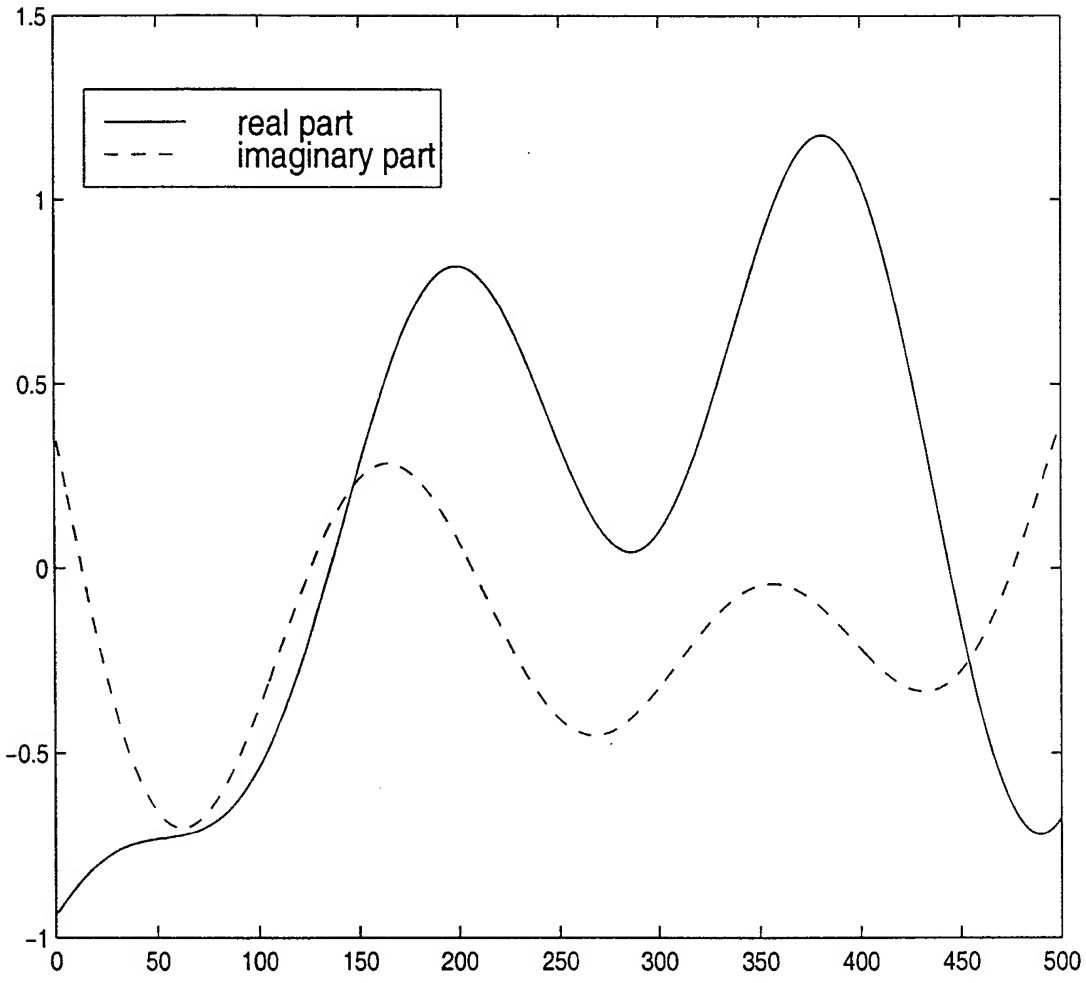
real part
imaginary part
1.5
1
0.5
0
-0.5
-1
0
50
100
150
200
250
300
350
400
450
500

Fig. 3

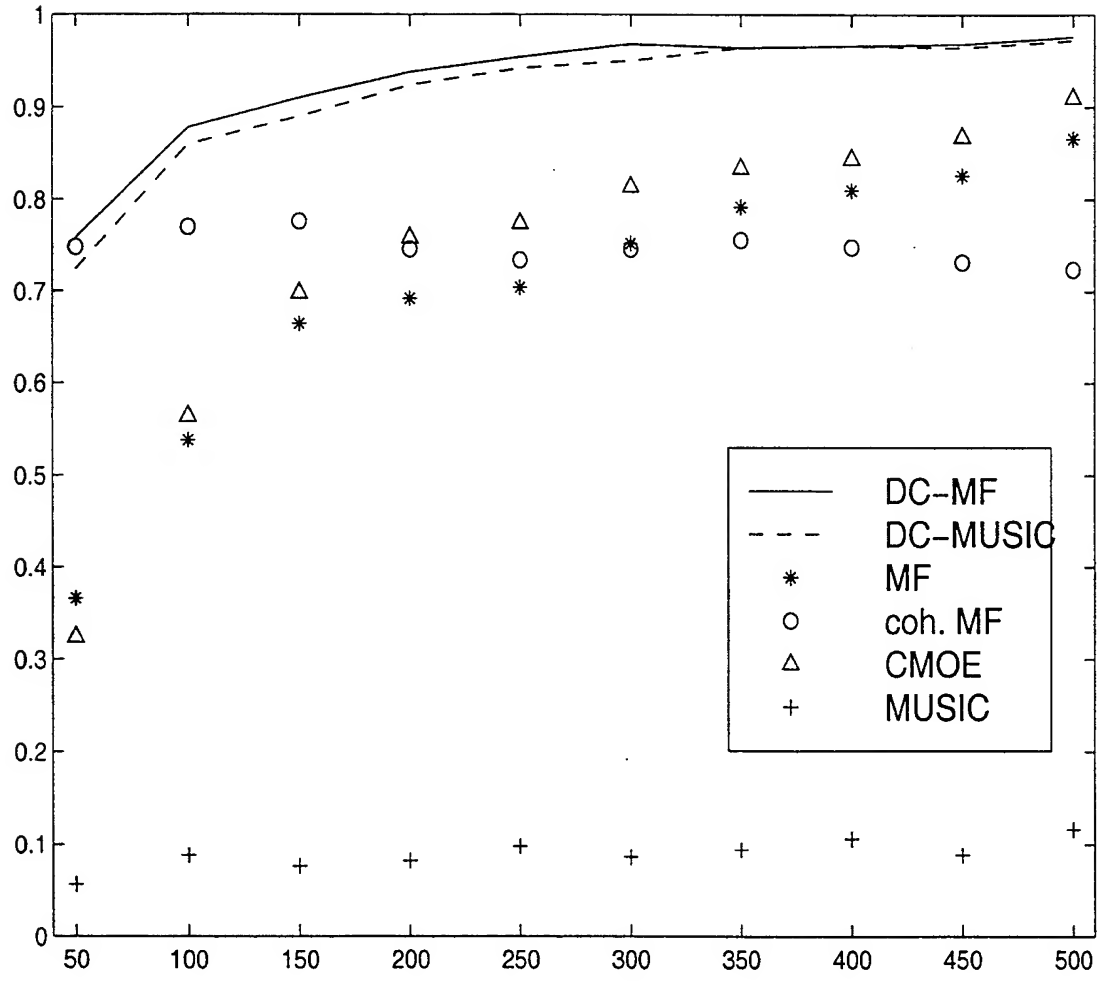
1
0.9
0.8
0.7
0.6
0.5
0.4
0.3
0.2
0.1
0
50
100
150
200
250
300
350
400
450
500
DC-MF
DC-MUSIC
MF
coh. MF
CMOE
MUSIC

Fig. 4

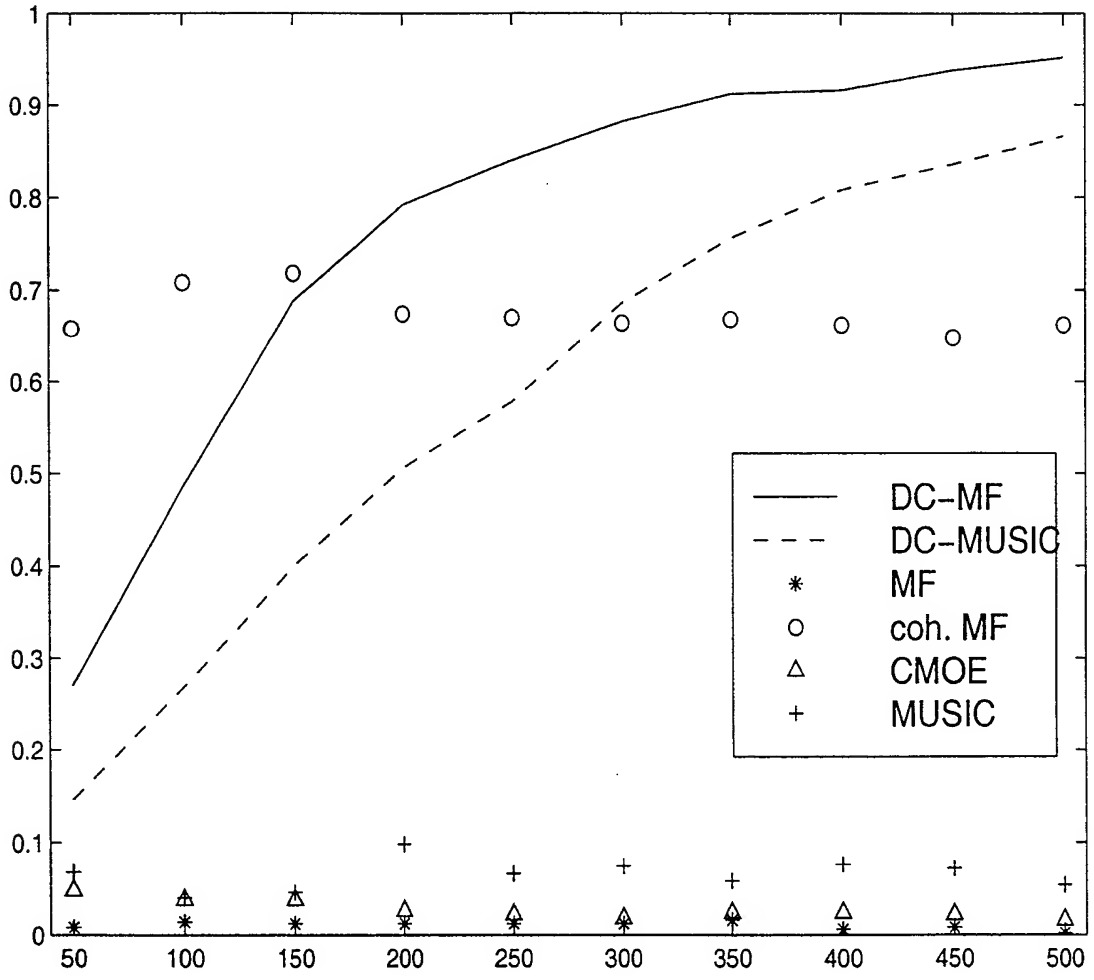
1
0.9
0.8
0.7
0.6
0.5
0.4
0.3
0.2
0.1
0
50
100
150
200
250
300
350
400
450
500
DC-MF
DC-MUSIC
MF
coh. MF
CMOE
MUSIC

Fig. 5

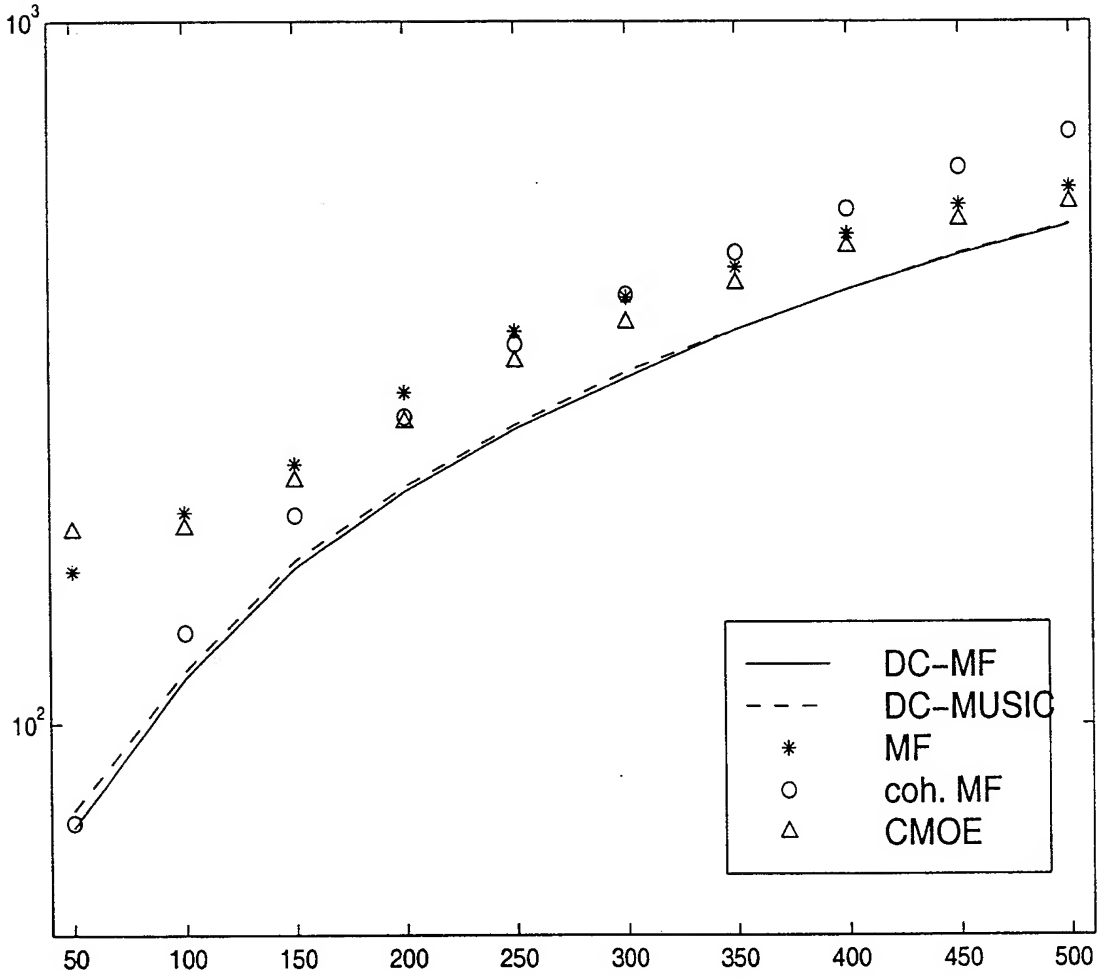
10^3
10^2
50
100
150
200
250
300
350
400
450
500
DC-MF
DC-MUSIC
MF
coh. MF
CMOE

Fig. 6

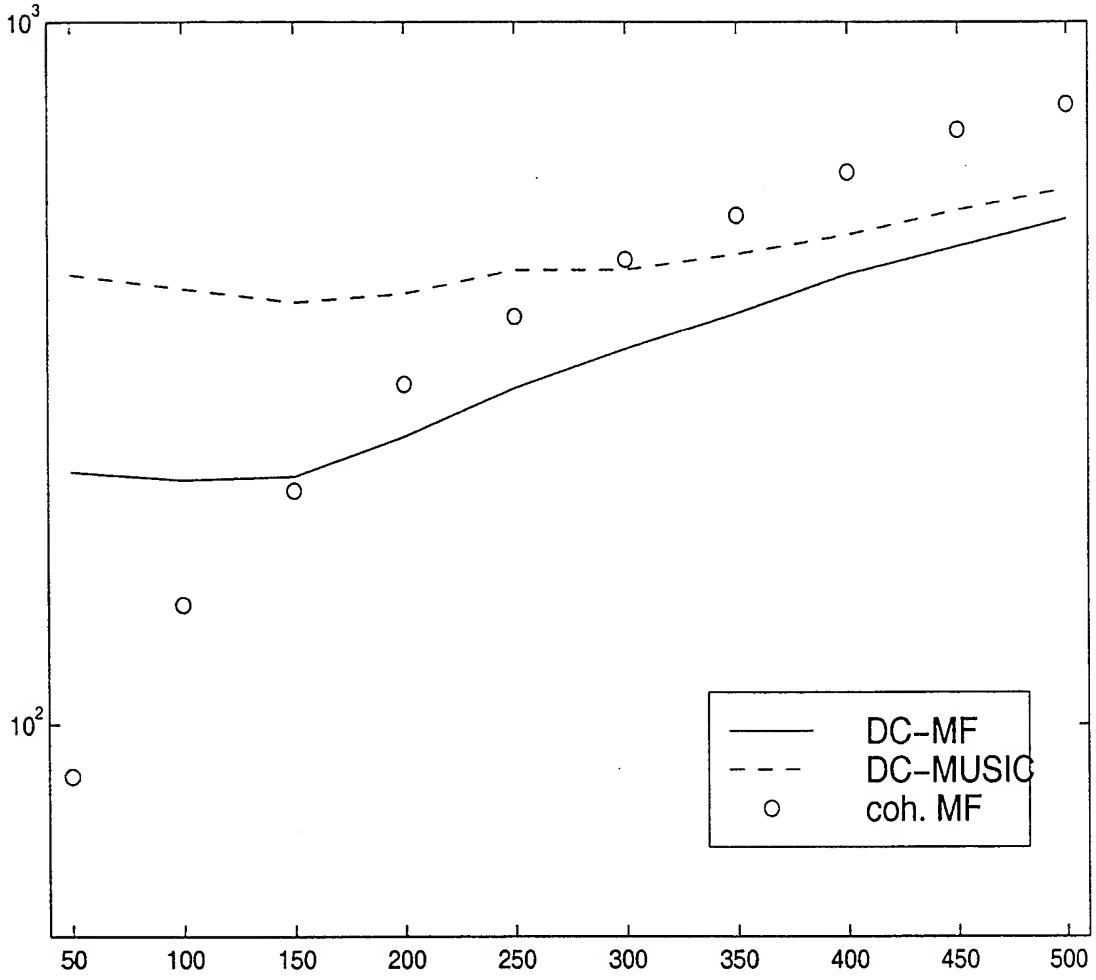
10^3
10^2
50
100
150
200
250
300
350
400
450
500
DC-MF
DC-MUSIC
coh. MF

Fig. 7

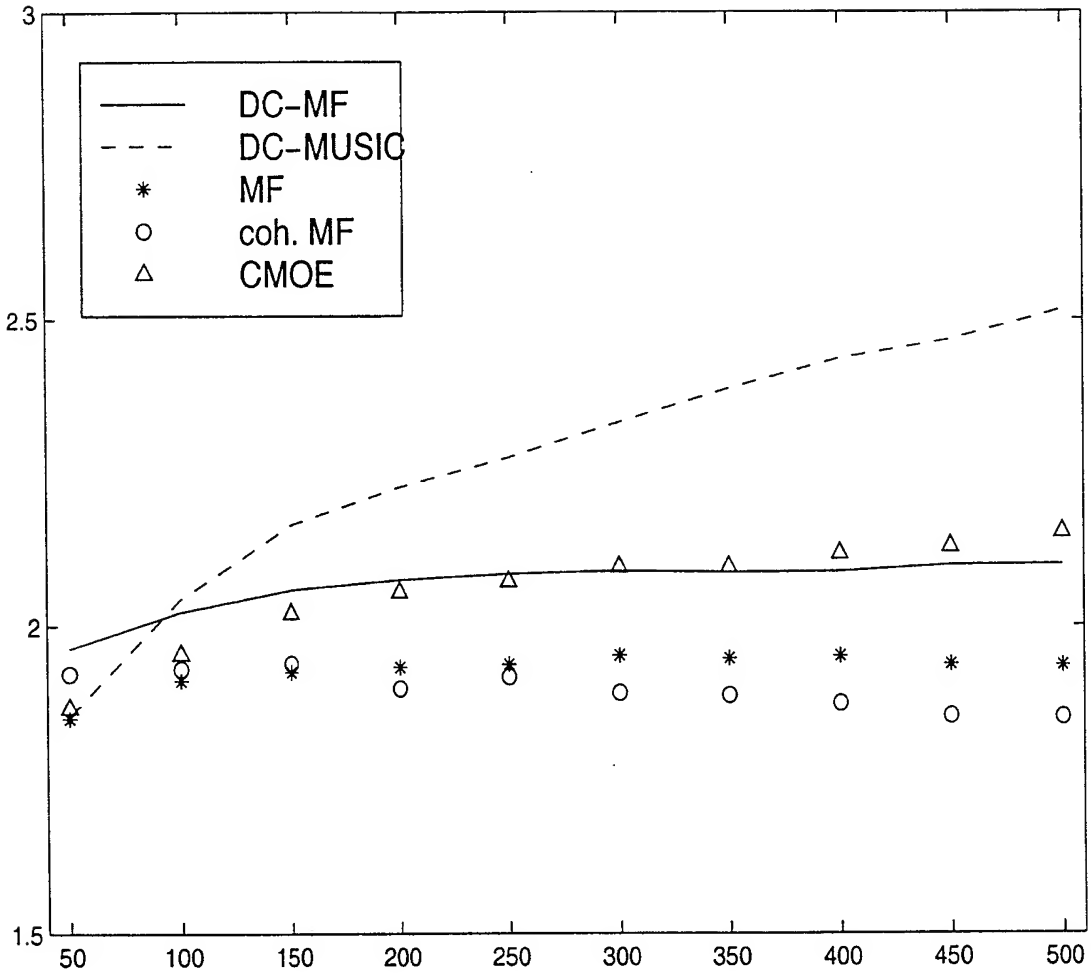
DC-MF
DC-MUSIC
MF
coh. MF
CMOE
3
2.5
2
1.5
50
100
150
200
250
300
350
400
450
500

Fig. 8

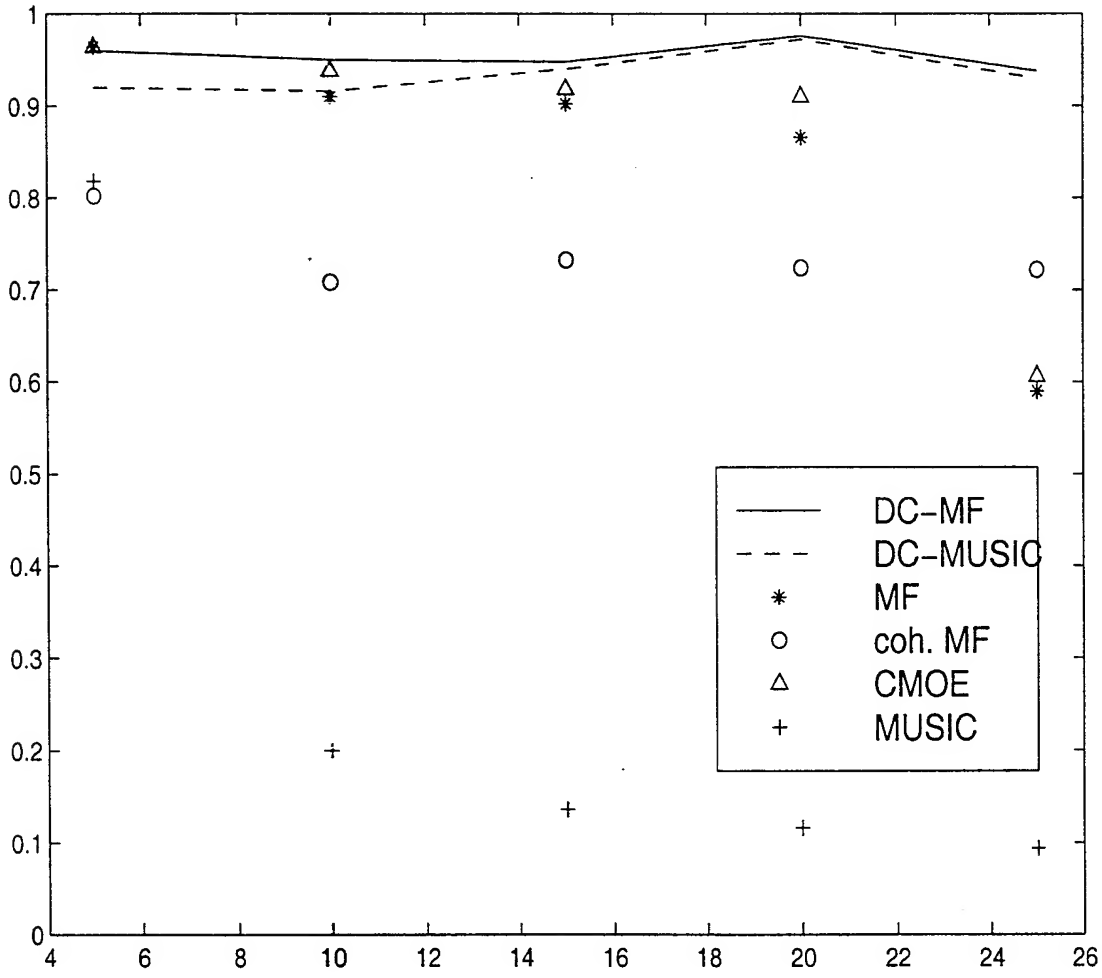
1
0.9
0.8
0.7
0.6
0.5
0.4
0.3
0.2
0.1
0
4
6
8
10
12
14
16
18
20
22
24
26
DC-MF
DC-MUSIC
MF
coh. MF
CMOE
MUSIC

Fig. 9

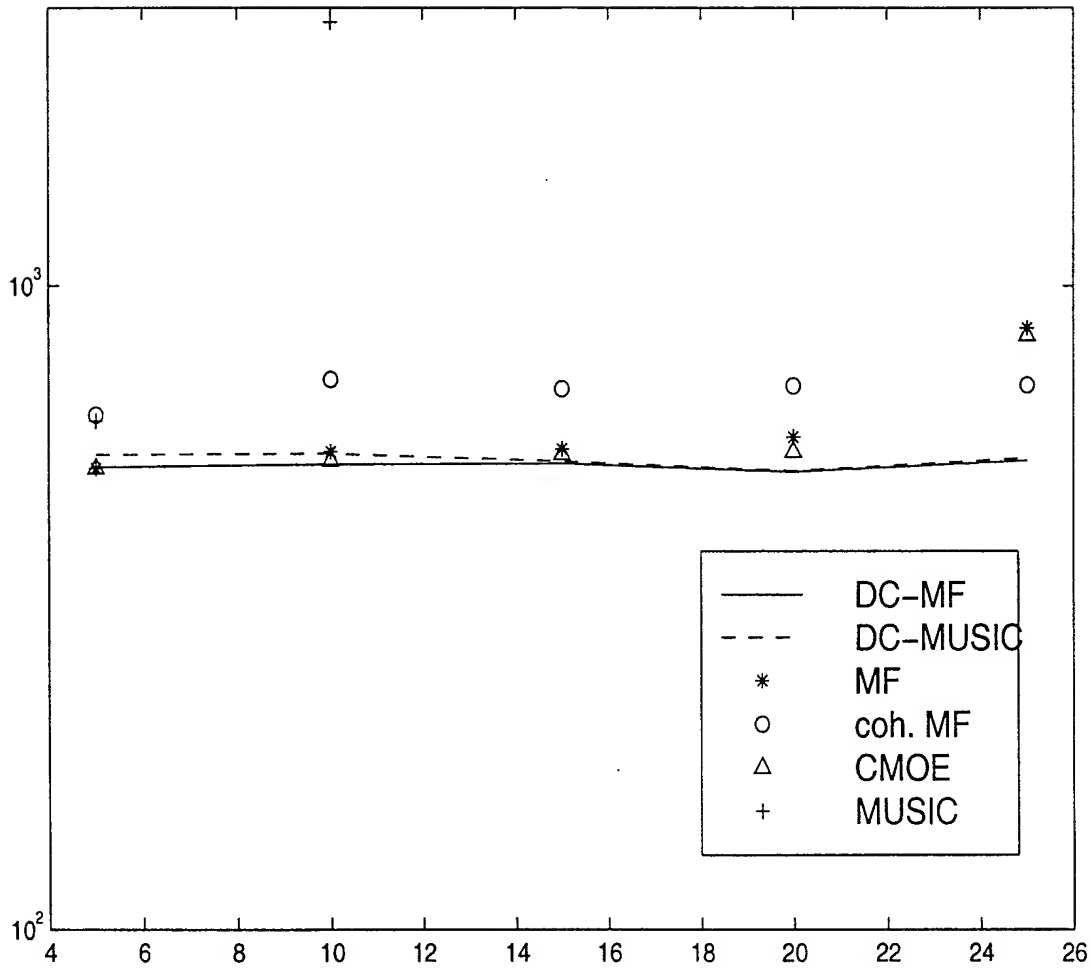
10^3
10^2
4
6
8
10
12
14
16
18
20
22
24
26
DC–MF
DC–MUSIC
MF
coh. MF
CMOE
MUSIC

Fig. 10

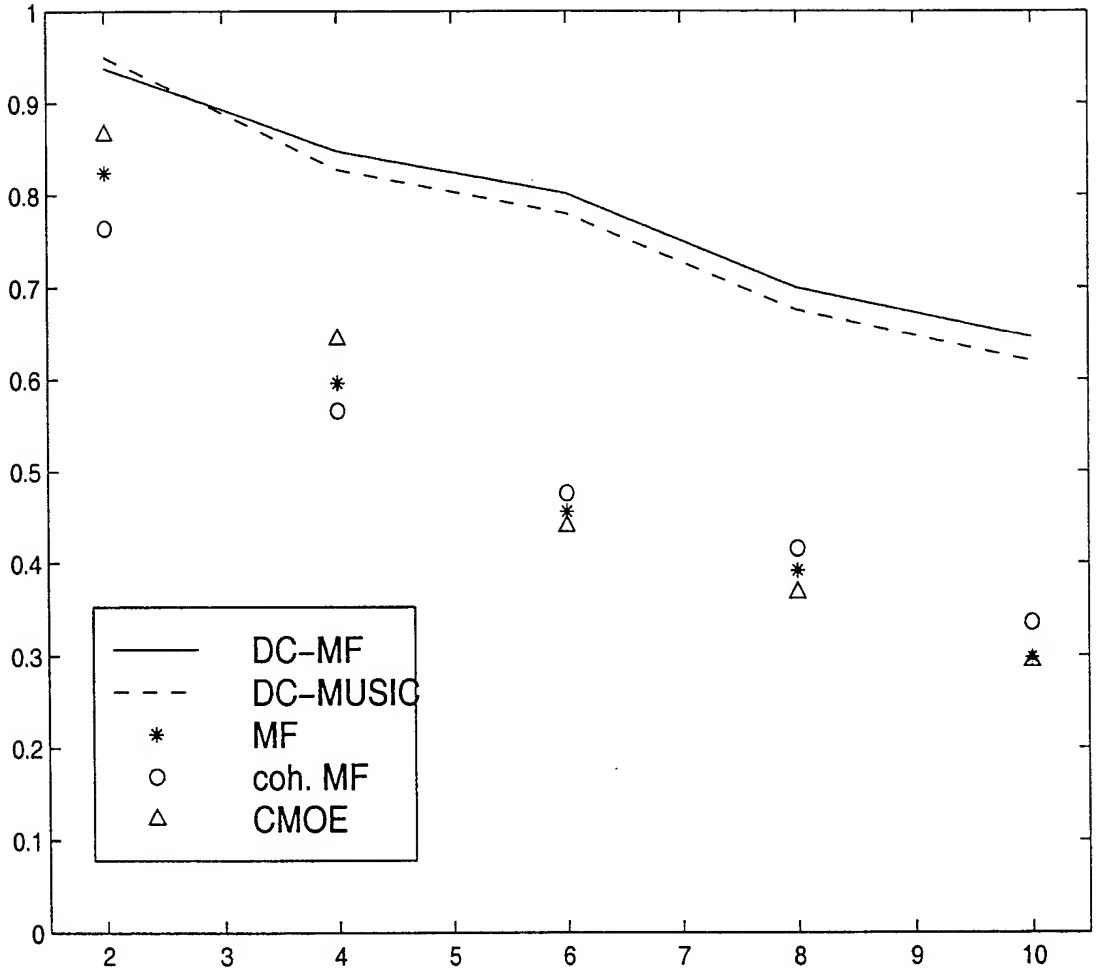
1
0.9
0.8
0.7
0.6
0.5
0.4
0.3
0.2
0.1
0
2
3
4
5
6
7
8
9
10
DC-MF
DC-MUSIC
MF
coh. MF
CMOE

Fig. 11

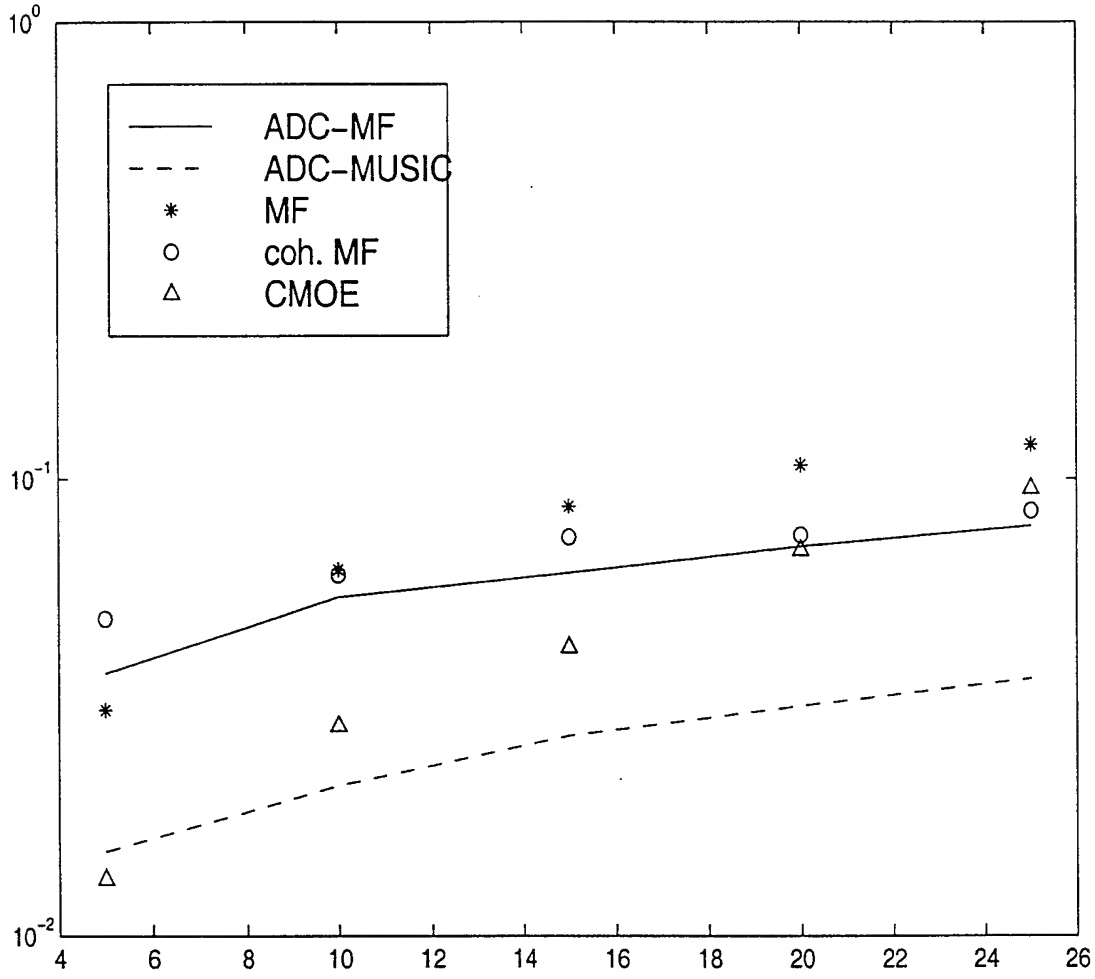
ADC-MF
ADC-MUSIC
MF
coh. MF
CMOE
10^0
10^{-1}
10^{-2}
4
6
8
10
12
14
16
18
20
22
24
26

Fig. 12

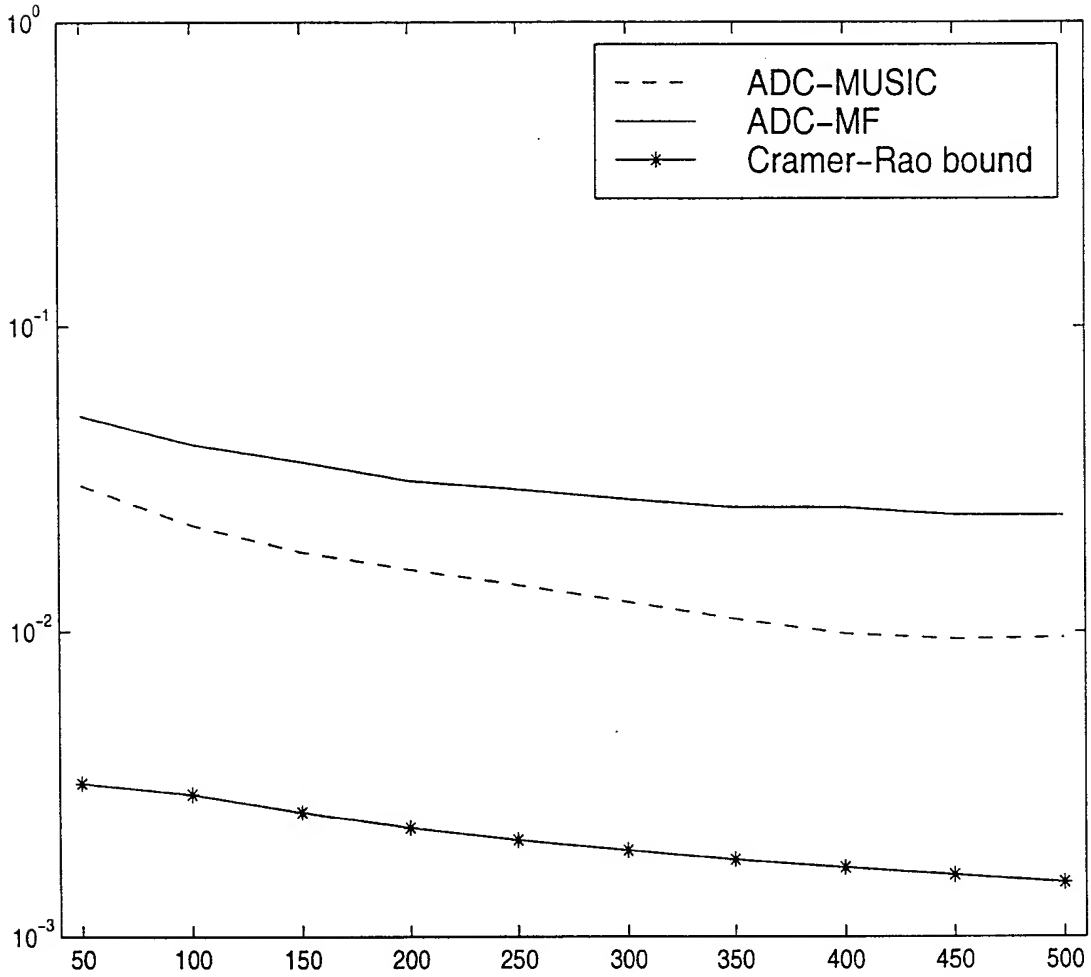
ADC-MUSIC
ADC-MF
Cramer-Rao bound
10^0
10^{-1}
10^{-2}
10^{-3}
50
100
150
200
250
300
350
400
450
500

Fig. 13

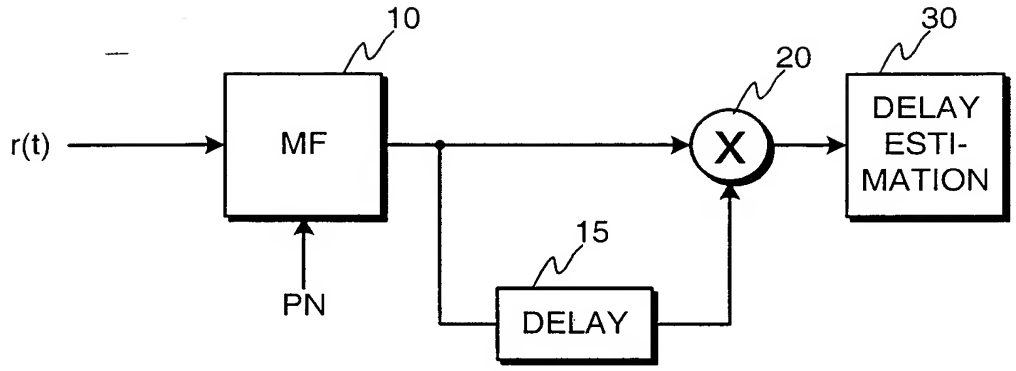
10
30
20
r(t)
MF
X
DELAY ESTI-MATION
15
PN
DELAY

Fig. 14

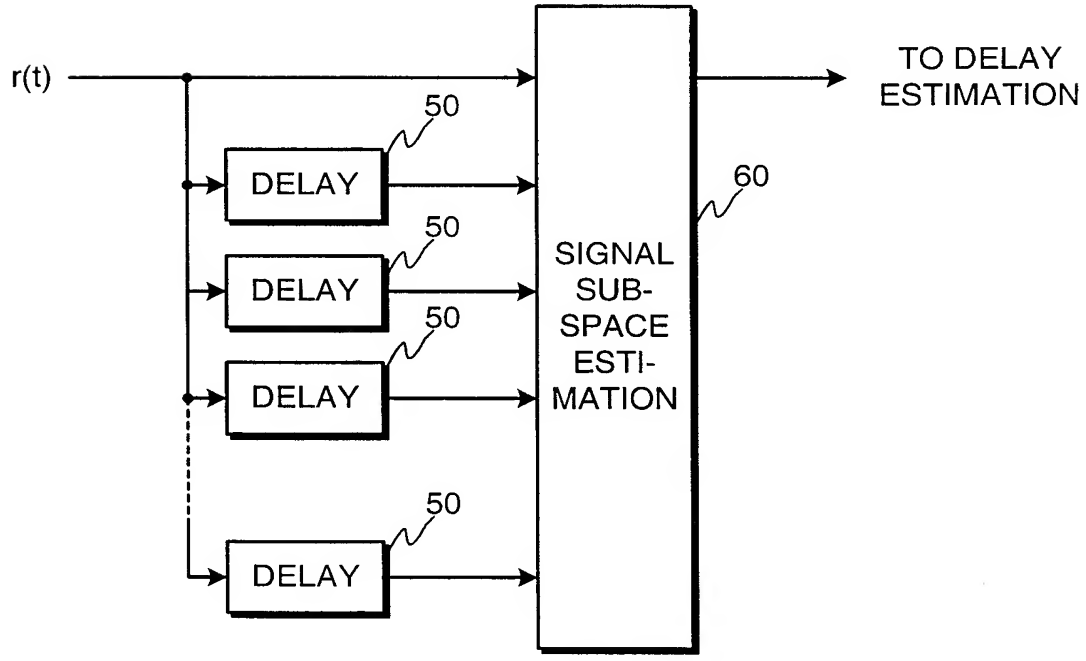
r(t)
TO DELAY ESTIMATION
50
DELAY
50
DELAY
50
DELAY
50
DELAY
60
SIGNAL SUB-SPACE ESTI-MATION

Fig. 15